

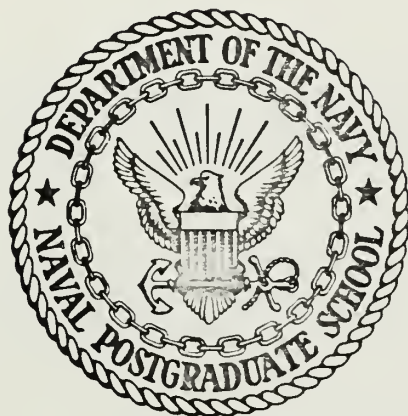
SOME CHARACTERISTICS OF A PROPULSIVE  
WATER JET

James Alexander Wilson



# NAVAL POSTGRADUATE SCHOOL

Monterey, California



## THESIS

SOME CHARACTERISTICS OF A PROPULSIVE  
WATER JET

by

James Alexander Wilson, Jr.

Thesis Advisor:

R. H. Nunn

December 1971

*Approved for public release; distribution unlimited.*



Some Characteristics of a Propulsive Water Jet

by

James Alexander Wilson, Jr.  
Lieutenant Commander, United States Navy  
B.S., Ch.E., Tufts University, 1960

Submitted in partial fulfillment of the  
requirements for the degree of

MASTER OF SCIENCE IN MECHANICAL ENGINEERING

from the

NAVAL POSTGRADUATE SCHOOL  
December 1971



## ABSTRACT

To obtain a high velocity, coherent, propulsive water jet, proper nozzle design is required. Existing high performance nozzles are considered, and a selected design is tested to provide optimization and performance data in the form of velocity and thrust loss with increasing jet stand-off. An expression is developed to predict the velocity loss using an empirical friction factor value determined from the data.





## TABLE OF CONTENTS

I.	INTRODUCTION -----	5
II.	STATEMENT OF THE PROBLEM -----	9
	A. RESEARCH OBJECTIVES -----	10
III.	LITERATURE SURVEY -----	12
IV.	TEST FACILITY DESCRIPTION -----	19
	A. DESIGN CONSIDERATIONS -----	19
	B. NOZZLE DESIGN -----	23
	C. BUCKET DESIGN -----	25
	D. INSTRUMENTATION -----	26
V.	TEST PROCEDURES -----	28
VI.	DISCUSSION OF RESULTS -----	30
	A. PHYSICAL RELATIONSHIPS -----	30
	1. Nozzle -----	31
	2. Bucket -----	31
	B. NOZZLE OPTIMIZATION -----	33
	C. PHOTOGRAPHIC RESULTS -----	40
	D. ANALYTICAL RESULTS -----	42
VII.	SUMMARY -----	45
	A. CONCLUSIONS -----	45
	B. RECOMMENDATIONS -----	46
	APPENDIX A - JET VELOCITY LOSS ANALYSIS -----	48
	BIBLIOGRAPHY -----	60
	INITIAL DISTRIBUTION LIST -----	61
	FORM DD 1473 -----	62



## ACKNOWLEDGEMENT

The author wishes to express his gratitude to Professor R. H. Nunn for his advice, encouragement and patience during the research, and to his wife, Ann, for her inspiration and the many hours she sacrificed.

A special note of thanks goes to the Mechanical Engineering Shop personnel, who assisted in the design of and constructed the test facility.



## I. INTRODUCTION

High speed mass transit systems are rapidly becoming a requirement to accommodate the transportation needs of cities and suburban areas. Current designs offer small to moderate increases over conventional railroad transportation, but future speeds of over 200 miles per hour are envisioned.

When these high speeds are considered, propulsion by driving wheels is ruled out because of traction limits, and propeller or jet engine thrust is unattractive because of the attendant noise and fumes. Additionally, the physical size and weight of onboard equipment to attain these speeds becomes a problem. Unconventional systems being seriously researched are linear induction and pressure-differential "transit tubes".

Another concept, proposed by Beckwith [Ref. 1], is that of hydraulic propulsion. It is essentially a linear hydraulic impulse turbine using high velocity water jets as the power fluid. The jet nozzles would be fixed in the roadbed and impinge on buckets mounted on the underside of the vehicle as shown in Fig. 1. Expended water would be collected in a trench and recycled, thereby minimizing overall water consumption. For a 150,000 pound, 200 passenger, streamlined vehicle capable of 250 miles per hour, a full-speed propulsive force of 3,700 pounds is required. This assumes an aerodynamic drag coefficient of 0.3 and



air cushion support for the vehicle. The propulsive force can be obtained with a water jet velocity of twice the vehicle speed, or 500 miles per hour, thus allowing expended water to "drop" into the trench at zero velocity. The pressure needed is 3620 psi, and allowing for 80 per cent efficiency of the nozzles, five nozzles of 0.125 in.<sup>2</sup> area each would be required per train length. At passenger terminals, a much higher thrust is needed for startup and acceleration. Assuming an acceleration of 0.5 g, a force of 75,000 lbs. is required. This would be accomplished by increasing the number of nozzles and taking advantage of the higher thrust per nozzle for vehicle speeds below 250 miles per hour. For example, at half speed the thrust is 1-1/2 times that at full speed; when stationary, it is twice the full speed thrust.

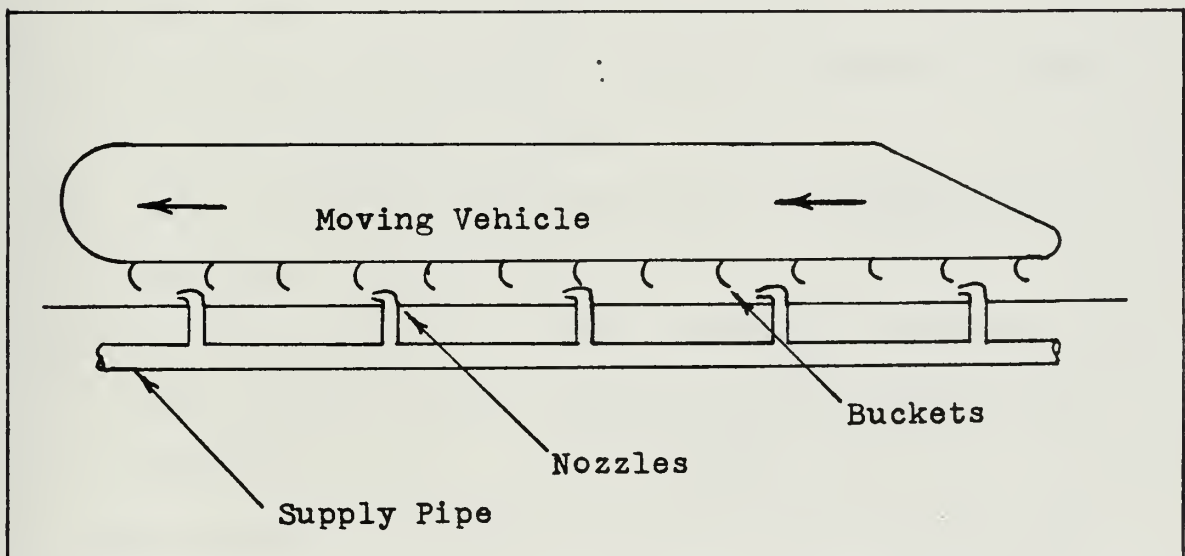


Fig. 1: Proposed Propulsion System (after Ref. 1)





Water would be supplied by pumping stations spaced every 30 miles and connected by six or seven in. high pressure piping. By providing an air "accumulator" for energy storage in the form of large diameter piping of sufficient length, pumps could be rated for continuous operation and would require two 3500 horsepower pumps per station for one-way train service. For two-way service, station spacing would be 15 miles apart. Pressure losses are estimated at 10 per cent, but cross connection between stations would help reduce these losses.

Advantages of the overall concept cited by the proposer are:

1. No onboard propulsion equipment, thus greatly reducing overall vehicle weight. Air cushion support would be on each vehicle.
2. Low vehicle noise and exhaust emission compared to propellers or jet engines.
3. Existing, commercially available equipment is used for the propulsion system.
4. Large "moving-to-stationary-part" clearances are permitted.
5. A one-way capacity of 3300 passengers per hour; two-way capacity of 6600 (pumping stations at 15 miles spacing).

Development of an effective method of switching individual nozzles on and off is required. Timing is quite critical for this operation since at 250 miles per hour, a 200 foot vehicle would pass one nozzle in a little more than 1/2 second.



Other likely problem areas in implementing the proposed design would be those of nozzle positioning relative to the vehicle's buckets, and the design of a nozzle to give high performance. These last two facets of the system were considered and studied to provide some insight into their possible design.



## II. STATEMENT OF THE PROBLEM

The description of the proposed transit system as a "linear hydraulic impulse turbine" provides a good image of the way in which the power fluid is used to drive the vehicles, yet there is an important difference in the manner in which the buckets receive the water jet. In normal turbine wheel applications, each bucket swings through an arc and is thus conveniently brought into line with the water jet axis. It then passes out of alignment just as the succeeding bucket swings into the jet axis.

For the linear case, unless the "track" is continuously curving, the buckets must pass across the axis of the water jet, which establishes a different set of requirements:

1. A shallow angle between jet axis and the direction of bucket travel is desired to obtain maximum thrust in the direction of travel. Conversely, steep angles would reduce thrust in the direction of travel and also give rise to considerable side forces. These are undesirable and, unless utilized to aid vehicle support, unusable.
2. Allowing for clearance between the moving buckets and the nozzle means that the jet will not contact the bucket until it has moved an appreciable distance beyond the nozzle. For example, a clearance of one in. and an angle of five degrees delays contact for 11.5 in.



3. The buckets should not pass directly above the nozzle, since the expended water will then drop into the path of the jet and interfere with it.

Based upon these requirements, the nozzles should be placed to the side of the buckets to allow expended water to drop free. This would give rise to side forces, which could be balanced by using four or six paired nozzles per vehicle, impinging on a double row of buckets. Also, a shallow angle requires that the jet travel over long distances in a coherent form, since any loss to spray or break-up results in loss of momentum and, therefore, vehicle thrust. Shorter jet travel could be obtained by closely spaced buckets; however, this would be uneconomical if proper nozzle design could provide the desired jet quality of coherence. Finally, a widely spreading jet cannot be tolerated since portions of it would not be properly turned by the bucket, resulting in inefficient bucket performance.

#### A. RESEARCH OBJECTIVES

The research was directed towards selecting and testing a nozzle design that would provide a jet which was stable and coherent over a long distance. Selection was made from successful designs in related high velocity water jet applications. To permit evaluation of the nozzle design, a testing facility had to be conceived and built. Within the limits of equipment and resources available, the research was to be scaled to match actual conditions of the proposed





transit system. When a jet of the required coherence had been obtained, its performance was to be compared with that predicted by a simplified mathematical model.



### III. LITERATURE SURVEY

Having specified the scope of the research, the literature was consulted to determine if previous studies of high velocity propulsive water jets had been conducted. None were found, but a closely related field - water jet cutting of rock and coal - yielded a number of interesting and useful articles. Nearly all of these stressed the importance of proper nozzle design to obtain the best performance of the water jet in cutting operations, yet different designs were claimed to do the best job.

Leach and Walker [Ref. 2] studied the performance of various nozzle configurations with a 1.0 mm exit diameter. Driving pressures were 130 atm (1910 psi) and 600 atm (8820 psi), provided by a high pressure pump in continuous operation. Testing was also done at a pressure of 5000 atm (73,500 psi), provided by a pressure intensifier arrangement. After preliminary testing of nozzles of widely differing internal geometry, they found that a conical contraction followed by a straight section of constant diameter had the best performance. Variations of the geometry of this design were then further investigated to optimize the contraction angle of the cone, the sharpness of internal corners of the cone entry and exit, and the straight section length to diameter ratio.

It was found that a cone angle between  $6^\circ$  and  $20^\circ$  with sharp corners at the cone entry and exit yielded the best



results in terms of jet stagnation pressure at a distance divided by driving pressure. Optimization of the length of the straight section showed a dramatic increase in performance for a length to diameter ratio of about three. With their best design - diameter one mm, length of straight section 2.5 mm, and cone angle  $13^\circ$  - Leach and Walker showed only a 20 per cent loss at approximately 150 diameters distance from the nozzle. Flow Reynolds numbers for these final results were  $Re_d = 1.79 \times 10^5$  and  $3.85 \times 10^5$ , where  $Re_d = \frac{u_0 d_0}{\nu}$ ,  $u_0$  = initial jet velocity,  $d_0$  = nozzle exit diameter, and  $\nu$  = kinematic viscosity of the fluid.

Subsequent tests varied the viscosity and surface tension of fluids tested to determine their effects. Polymer solutions of 1/4 per cent and 1/2 per cent boosted performance appreciably at all distances. A detergent solution gave improved results at distances greater than 250 nozzle diameters.

Another important observation by Leach and Walker was that the appearance of the jet was very misleading. In normal lighting the jet appeared very broken up, yet by backlighting and x-ray techniques their photographs showed that actually there was a coherent core containing the bulk of the fluid. This was surrounded by a fine mist or spray which was a small fraction of the fluid issuing from the nozzle.

Farmer and Attewell [Ref. 3] conducted a similar investigation for nozzles with an exit diameter of 1/16 in. (1.59



mm) at a pressure of 700 kg/cm<sup>2</sup> (9954 psi). Seven designs were evaluated on the basis of how far the free jet would conduct an electric current, thus obtaining the breakup length of the jet. The reasoning was that the longer the jet remained continuous, the more efficient the nozzle design. Three of these nozzles had an inside contour matching the streamlines of potential flow for contraction angles of 70°, 60°, and 40°. No straight section followed the contraction. These three had breakup lengths of 0.60, 0.55, and 0.65 m respectively. Another design, a simple 20° cone without any straight section, and with sharp corners at the cone entry, had a breakup length of 0.60 m. This nozzle was their selection for further study in rock cutting, apparently because of its simplicity in manufacture. One nozzle of the cone-and-straight-section type was tested and performed poorly, with a breakup length of only 0.25 m. The straight section length was not given, but the cone angle was 45°, a rather abrupt contraction.

Larger scale testing of high velocity water jets has been conducted by the U. S. Bureau of Mines and reported by Palowitch and Malenka [Ref. 4]. These tests were made at pressures of 3000 and 4000 psi, using nozzles of 3/8 in. and 5/32 in. diameter. Five different designs were tested to obtain the pressure distribution in the free jet at a distance of 12 in. from the nozzle. The best performance was obtained with a 22.5° cone shape followed by a straight section that was 1.125 in. long (three diameters). The





pressure profile obtained with this nozzle at a 12 in. standoff shows the jet to be concentrated within a diameter of about 0.8 in. It gave a peak pressure of about 3000 psi compared with a peak of 2400 psi for the second best design. This nozzle design was used in actual mining tests that followed.

Successful results with the cone and straight section design were reported by Harris [Ref. 5] in tests conducted at pressures of 10,000 psi, 30,000 psi and 50,000 psi, with nozzle exit diameters ranging from 0.002 in. to 0.010 in. These were used in a research program conducted by the National Research Council of Canada to determine the feasibility of cutting various materials commercially with water jets. Further research in the range of 70,000 to 100,000 psi was planned and the nozzle design was considered adequate for these purposes.

Oak Ridge National Laboratory has also instituted a testing program for rock tunnel excavation by high pressure water jets. The nozzles selected for these studies were of the cone and straight section design, using a  $13^\circ$  cone contraction angle and a straight section length of 2.5 times the nozzle exit diameter [Ref. 6].

Rouse, et al, [Ref. 7] investigated methods of improving fire monitor performance under a U. S. Navy contract with the Iowa Institute of Hydraulic Research for a number of years. Extensive facilities for full scale testing were established and attention was focused on nozzle design and



turbulence reduction in fire monitors. Nozzle exit diameters ranged from 1.5 to 3 in. and water pressures ranged from 50 to 200 psi.

The authors pointed out that all turbulence cannot be eliminated but, as a minimum, the scale of turbulence can be reduced by honeycomb installation in the monitor barrel and by flow guide vanes at its bends. In firefighting applications these flow straighteners are subject to fouling and thus could not have very narrow passages. However, improvement was found to occur in the stream stability even by using the large passage flow guides.

With respect to nozzle design, it was considered most important to eliminate sharp corners and abrupt transitions in the contraction region. In addition, the authors considered that any cylindrical section following the contraction would contribute to the turbulent eddies through boundary layer effects, and thus concluded that this should be eliminated, or at least minimized. A series of different nozzles based on the foregoing design criteria were tested. These were systematic variations between a plain orifice and a  $7^\circ$  cone, producing a jet of 1.5 in. at the vena contracta. A second series of nozzles with cylindrical sections at the exit and curved contraction regions of different radii of curvature was also tested. These had a 1.5 in. exit diameter and the contraction angle varied from  $45^\circ$  to  $7^\circ$ .

Comparison between nozzles was made by a sampling technique to obtain the jet concentration pattern at a given



distance. The best performing nozzle was one with a  $30^\circ$  contraction angle, well rounded at the base, and without a cylindrical section at the exit. This design was subsequently tested by Leach and Walker [Ref. 2], but it did not perform as well as did the cone and cylinder profile.

In reviewing the studies quoted, there are three nozzle designs which, according to the researchers concerned, perform best with respect to jet coherence and stability. The methods and criteria for evaluating these three were all different, as were the flow parameters in terms of the Reynolds numbers obtained. An additional consideration in selecting one of these is the ease of manufacture if a large number of nozzles were to be produced for high pressure applications.

Figure 2 shows the three superior nozzle designs, and Fig. 3 presents the Reynolds number ranges covered by the investigators quoted, including the present study.



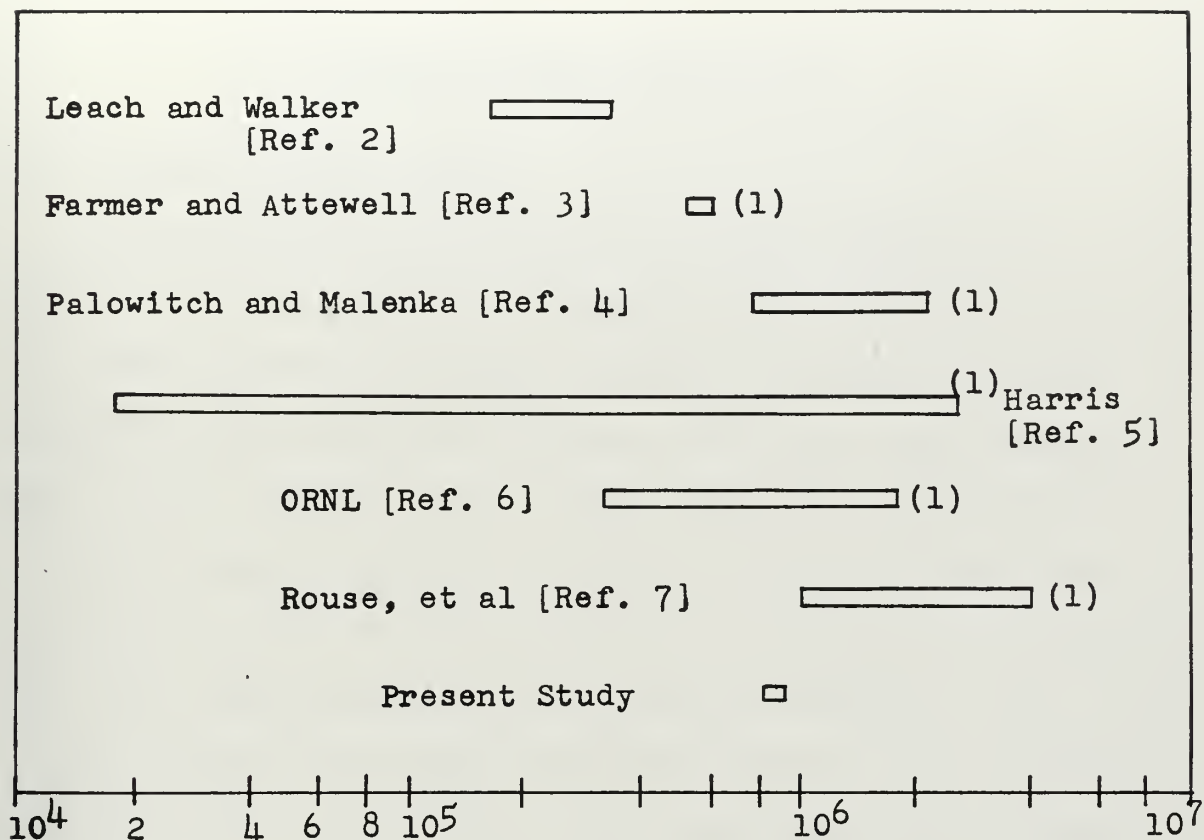


Fig. 2: High Velocity Water Jet Reynolds Number Ranges  
 Note: (1)  $Re_d$  estimated from pressures cited

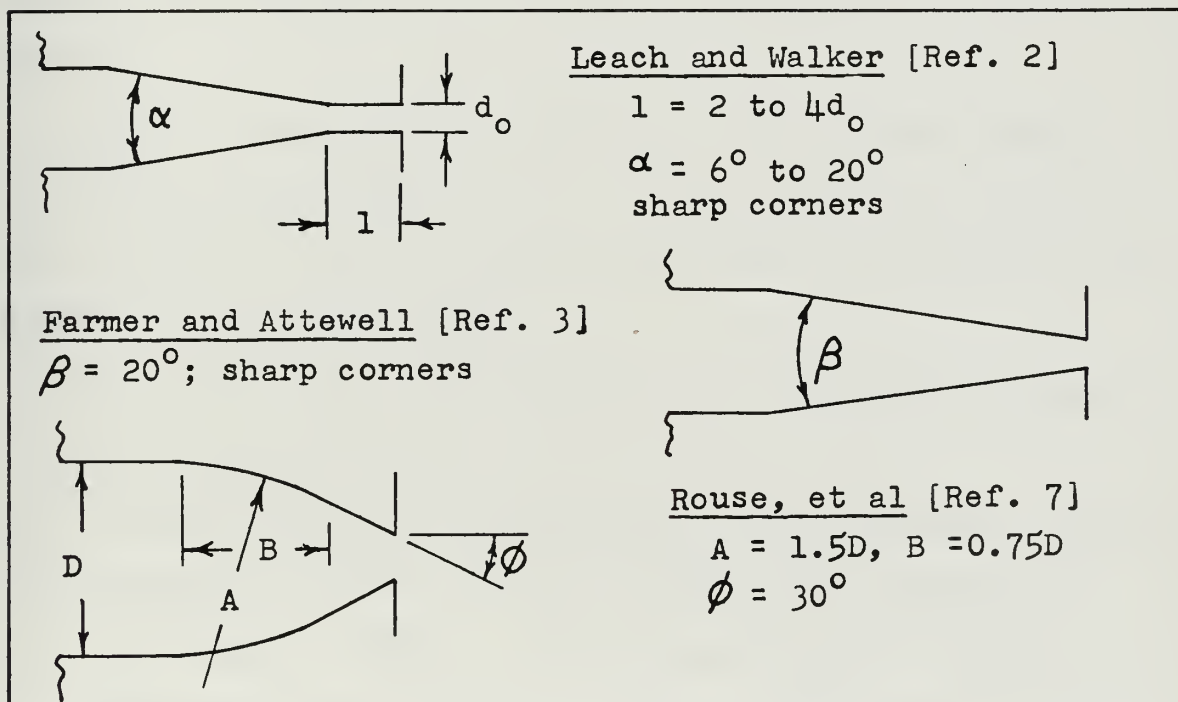


Fig. 3: High Performance Nozzle Profiles





#### IV. TEST FACILITY DESCRIPTION

##### A. DESIGN CONSIDERATIONS

Having established the need to select and test a nozzle that could produce a coherent propulsive jet, it was then necessary to adapt or construct a test facility to allow making meaningful measurements and evaluations. Most of the research cited in the literature concentrated on small diameter nozzles, primarily because of the rock cutting objective. It was considered important to verify that the design selected would perform properly at the larger diameter and higher Reynolds number of the proposed transit system. Therefore, full scale testing of a 0.400 in. diameter nozzle at 3620 psi was desired, as was the capability to check jet to bucket interaction in future studies.

Without considerable expenditures of time and funds, it quickly became apparent that these objectives could not be fully met. The following are the major constraints that affected the system design:

1. Limited funds - make maximum use of locally available materials.
2. Limited space for test facility and associated piping.
3. Highest pressure source available was from bottled nitrogen at 2000 psi via an existing multi-bottle manifold and a 0-1500 psi pressure regulator.



4. High flow rates required a fluid reservoir of substantial volume.

The test facility that was built is shown in Figs. 4, 5, 6, 7, and 8. It provides four degrees of motion for bucket positioning: parallel to the jet axis, transverse, vertical and rotational. The bucket assembly is secured in position by clamping and only stationary measurements are possible. Maximum nozzle to bucket distance is 98 in. The nozzle assembly is fixed and braced to prevent strain on the piping connections from reactive thrust. All piping is Schedule 80 seamless steel, rated for and hydrostatically tested to 2000 psi. The capacity of the four inch diameter reservoir piping is approximately one cubic foot, which permits a run time varying from 2.5 sec to 4.5 sec for head pressures of 1500 psi to 500 psi respectively.

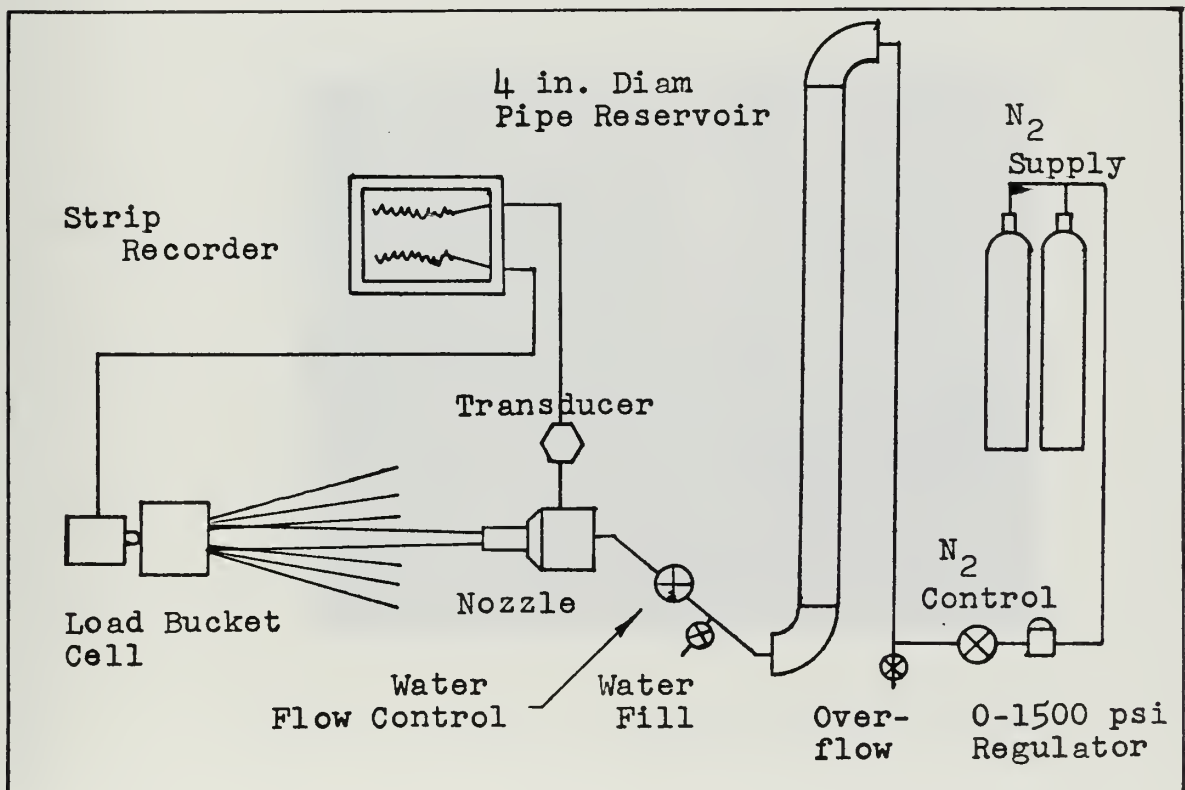


Fig. 4: Test Facility Schematic



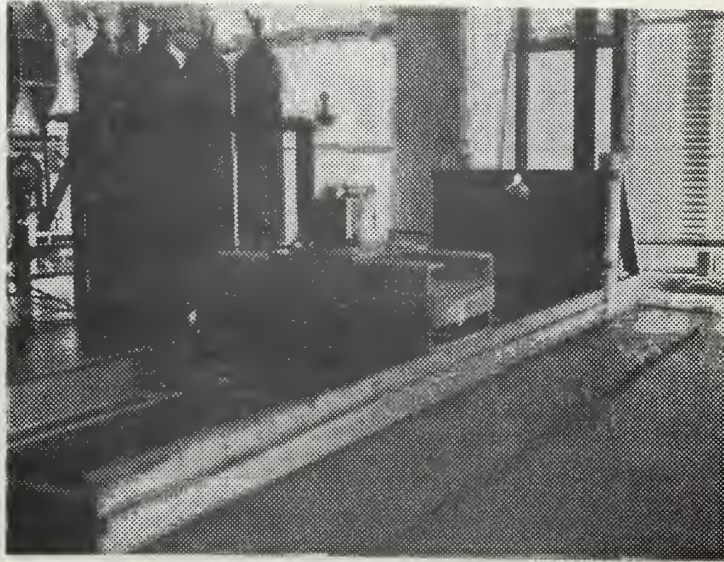


Fig. 5: Testing Facility



Fig. 6: Testing Facility With  
Spray Covers in Place





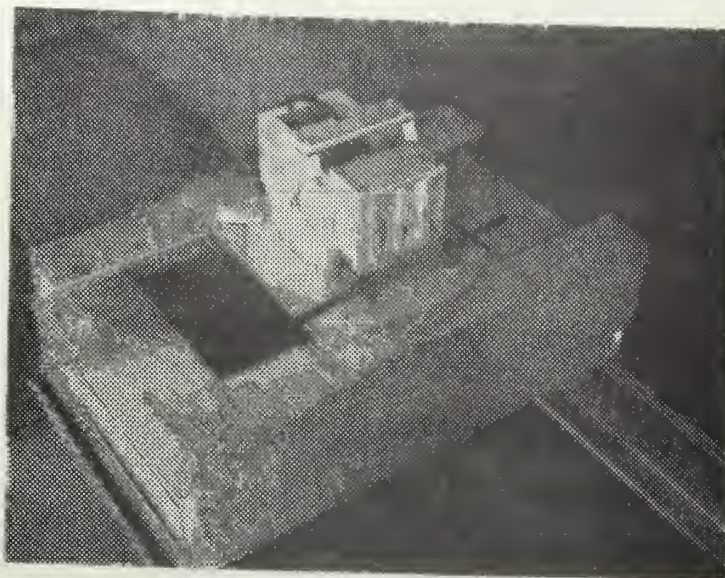


Fig. 7: Bucket Assembly

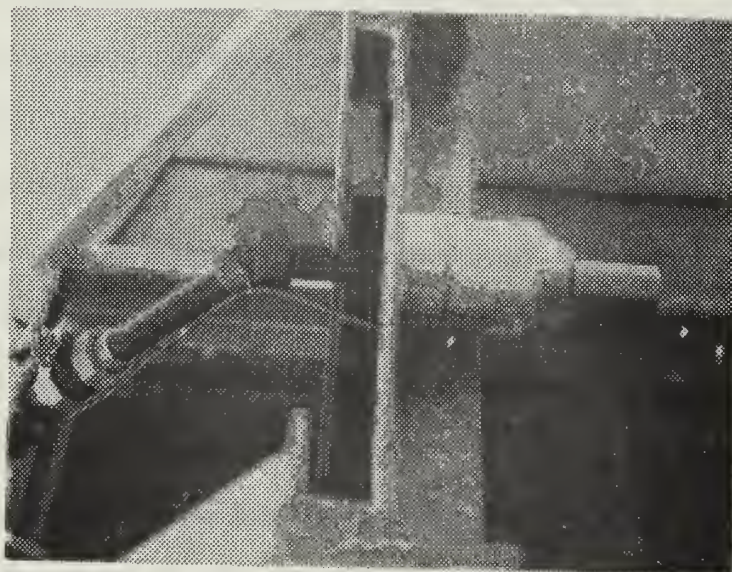


Fig. 8: Nozzle and Nozzle Block





A one inch manually operated ball valve controls the water flow to the nozzle. Nitrogen flow is controlled by either a manually operated or a solenoid operated one inch ball valve. One-quarter inch high pressure globe valves are used for water filling and overflow as well as system drainage.

Two plywood covers contain the water spray during operation and are fitted with plexiglass panels to permit observation of the jet. The covers slide in and are supported by angle iron attached to the outside of the axial rails.

#### B. NOZZLE DESIGN

The three nozzle designs shown in Fig. 3 were considered for their suitability in achieving the coherent jet needed for propulsive use. Since all three were claimed to give a coherent, stable property to the water stream, the most desirable method would have been to conduct tests of the three designs to evaluate which one had the best performance. Time limitations, however, required that only one be selected on the basis of existing information.

The profile recommended by Rouse, et al, [Ref. 7] was discarded because it had been developed using low pressures and, when this design was used by Leach and Walker [Ref. 2] in preliminary evaluations, it did not perform as well as the cone and cylinder nozzle profile. It should be noted that, while the two investigations had a forty-fold difference in pressure, the Reynolds numbers differed by only approximately



three-fold because of the diameters used. Farmer and Attewell [Ref. 3] proposed the  $20^\circ$  cone without any cylindrical section, yet shapes similar to this ( $6^\circ$  and  $13^\circ$  cones) gave inferior results when tested by Leach and Walker. The basis of evaluation was different for the two studies which may account for the difference in conclusions.

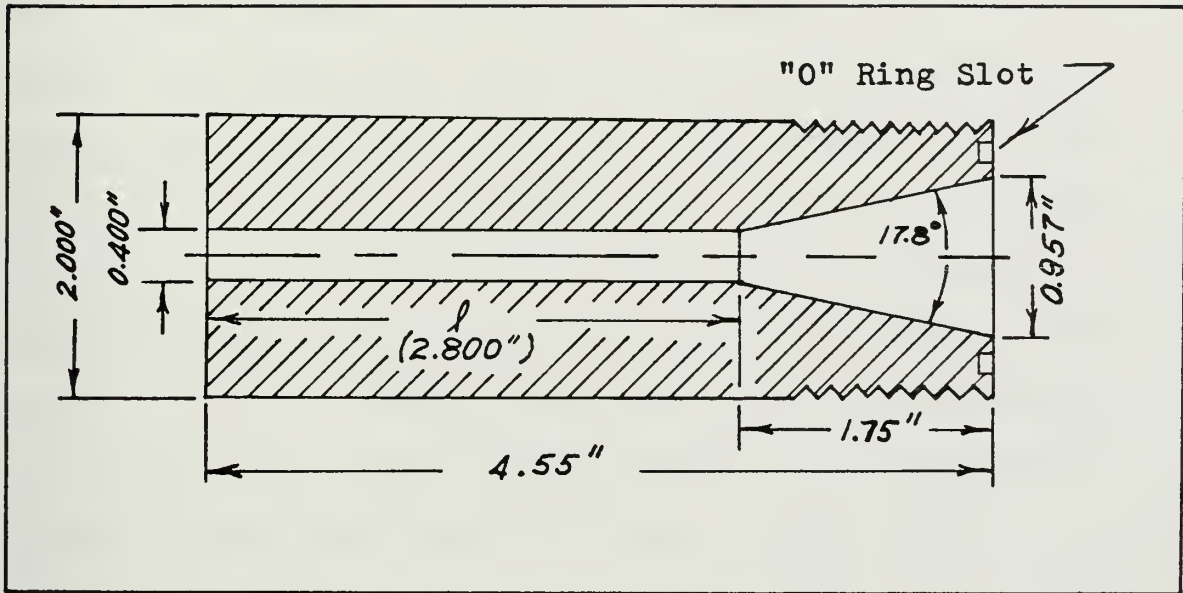


**Fig. 9 : Nozzle Details**

The cone and cylinder nozzle design was selected for use in the present study, and is shown in Fig. 9. In addition to the performance comparisons discussed above it had been successfully used in various high pressure projects with a wide range of Reynolds numbers and with nozzle diameters up to 0.375 in. [Palowitch and Malanka, Ref. 4]. Finally, it could be manufactured easily because of the simple geometry of its profile.

It was considered important to determine the optimum length of the straight section for the nozzle fabricated,



since the only studies of this effect were those of Leach and Walker [Ref. 2], whose nozzle had a 1 mm diameter. For this reason the nozzle was initially made with a straight section length of eight nozzle diameters. The material used was brass, and all internal surfaces were lapped and polished to a visually bright finish. The diameter at the base of the cone was matched to the inside diameter of the nozzle block. An O-ring seal was used to avoid the possibility of gasket protrusions into the flow. The nozzle block bore diameter was machined to match that of the one inch pipe threaded into it. Thus, a constant diameter straight section length of 26.25 nozzle diameters (10.5 in.) preceded the nozzle itself. A second nozzle was made with a matching profile but a straight section length of 11 diameters to obtain optimization data for longer nozzle lengths.

### C. BUCKET DESIGN

Various methods of gauging or measuring the jet coherence and nozzle performance were considered. Stagnation pressure would have given the most accurate measure of jet velocity, but the problem of valid measurements at positions where the jet had fully or partially broken up argued against this technique. Accurate positioning of a device such as a pitot tube or a plate with an aperture did not appear to be feasible with the equipment that could be built and with the intermittent operation that was necessary.

A more reliable and workable method appeared to be measurement of the thrust generated in changing the jet flow



direction by a bucket device. This had the disadvantage of adding a bucket efficiency error to the calculation of jet velocity, but it helped overcome the requirement for precise positioning to obtain a good measure of the velocity. Additionally, it was more closely related to the type of equipment which would be used in the proposed transit system. The Pelton bucket used in impulse turbines has a high efficiency and has evolved as the best shape to use for that application. Unfortunately, its profile would have been extremely difficult to fabricate with the shop facilities available. To simplify the design, yet accomplish the jet reversal, the bucket shown in Fig. 7 was conceived. It was machined from aluminum and has curved portions of 0.75 in. radii on 1.436 in. centers. The radii used were sized from the Pelton bucket dimensions given by Spannhake [Ref. 8] for a one inch jet. This larger size (one in.) was used to allow for jet spreading at a distance from the nozzle. It was realized that this design would introduce an inefficiency in conversion of jet momentum to thrust, but by comparing to an initial value of thrust at the nozzle exit, the error could be taken into account. The bucket block is supported by horizontal guides and is free to move within its receiver, thus transferring the thrust developed to a load cell mounted behind it.

#### D. INSTRUMENTATION

Measurement of the static water pressure just upstream of the nozzle was accomplished by a Daystrom 0-1500 psi variable reluctance type pressure transducer connected to





a pressure tap in the nozzle block. The pressure tap was one-eighth in. in diameter and was located one-half in. behind the base of the nozzle contraction cone. Thrust was measured by a 0-2000 lb capacity Baldwin Load Cell which consists of a strain gauge and bridge circuit assembly within a sealed container.

The pressure and thrust signals were recorded using a two-channel Hewlett Packard 1062A Carrier Amplifier and 7702B Recorder unit. Both sensors were checked for linearity and calibrated with their recording unit. A Volumetrics Co. Model QCE - 1 Portable Quick Disconnect Pressure Console was used for the transducer calibration, and a Baldwin Southwark Emery Universal Testing Machine, Serial Number 35430, was used for the load cell. The load cell accuracy was within 0.2 per cent for a 1000 lb. range; that for the transducer was within 1.0 per cent for a 700 psi range.



## V. TEST PROCEDURES

Initial trials indicated that for four full bottles of nitrogen, approximately ten runs could be made at a nozzle head pressure of 500 psi before the supply of gas was too low to maintain a constant value of thrust. For a head pressure of 500 psi, the theoretical velocity is 279 ft/sec and the flow Reynolds number is  $8.45 \times 10^5$ . Since this value is of the same order of magnitude as the Reynolds number for the investigation by Leach and Walker [Ref. 2], it was decided that this would be a useful level for conducting the nozzle optimization tests. This should permit comparison of new data with their results.

Runs were commenced with a nozzle length of seven diameters. Thrust and pressure were recorded for various values of nozzle to bucket distance. During initial runs, alignment of the bucket assembly with the jet axis was accomplished with a sighting device which fitted into the nozzle bore. This procedure was later discarded for the more direct and reliable method of operating the jet at low pressure and visually confirming that the jet impinged on the flow splitter of the bucket.

The sequence for each run was as follows: fill the four inch pipe reservoir to the point of overflow, ensuring that trapped air had been expelled from the system up to the nozzle exit; close drain valves and pressurize the system to the desired level; start the recorder and open the water



flow control valve; within two seconds, close the solenoid valve switch and allow the system to blow down excess pressure. This procedure yielded a steady value for the nozzle pressure for an average duration of about three seconds. Recorded values of thrust were irregular and fluctuating for downstream portions of the jet where significant jet breakup was observed, but quite smooth for runs close to the nozzle, as would be expected. The traces were visually averaged to obtain a value of thrust corresponding to a value of nozzle pressure.

After obtaining a set of runs at various bucket locations for a particular nozzle length, the nozzle was cut back to a new length. This was repeated until the straight section length was zero. This procedure was not wholly satisfactory, since any questionable runs could not be repeated once the nozzle was cut back. However, time did not allow the alternative of making up a series of nozzles of different lengths.

The jet obtained for various nozzle lengths was photographed to attempt to show its quality and make up. To accomplish this, the jet was fired into a box containing wire mesh screening to absorb the water, since the return spray of the bucket completely obscured the jet. Various lighting techniques and camera speed and shutter combinations were tried. The best pictures were obtained by a diffused back lighting with a shutter speed of  $1/500$ th sec. This technique gives a shadow effect where the water in the jet is concentrated. The film used was high contrast 4 x 5 in. Type 51 Polaroid, exposed in a Graflex camera using the focal plane shutter.



## VI. DISCUSSION OF RESULTS

### A. PHYSICAL RELATIONSHIPS

The basic measurements taken in the experimental investigations were that of nozzle block pressure ( $P_1$ ) and the thrust as measured at the bucket ( $F_m$ ). In subsequent paragraphs formulae are developed for relating the ideal jet thrust to  $P_1$ , and an approximate relationship is obtained for the reduced jet mean velocity at the bucket ( $u_2$ ) in terms of the measured variables.

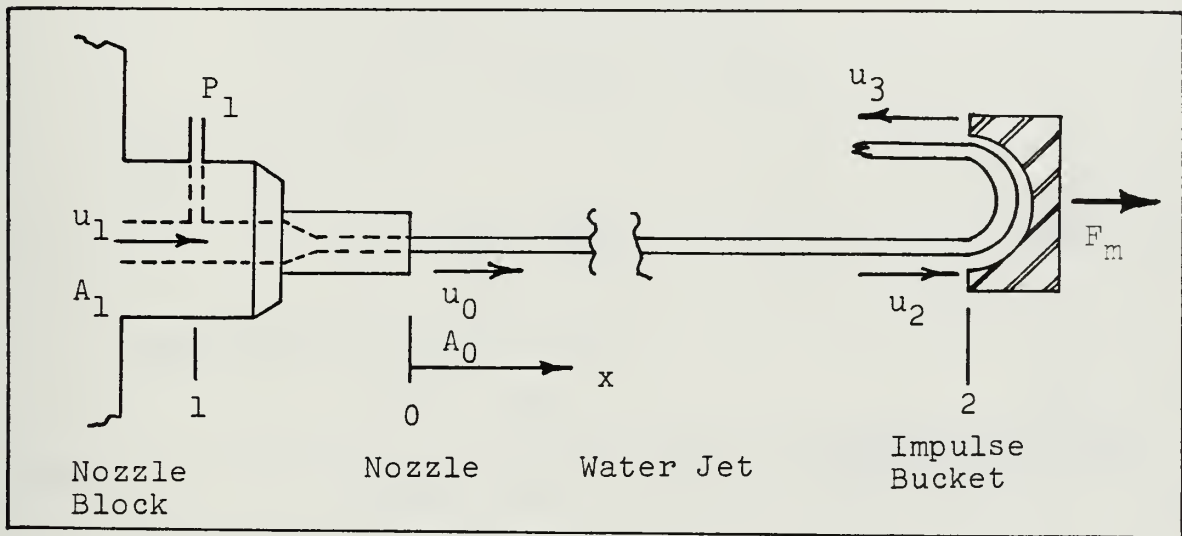


Fig. 10: Nozzle-Bucket Relationships

For the ideal situation it is assumed that the water density is constant and that the nozzle design is such that no velocity losses occur from the point of pressure measurement ( $P_1$ ) to the nozzle exit. The jet is assumed to suffer no loss in mass during its travel from the





nozzle exit to the bucket so that  $m_2 = m_0$ . Finally, it is assumed that the bucket reverses the flow with no loss so that for the ideal case  $u_3 = -u_2$ .

### 1. Nozzle

Application of the Bernoulli equation to the flow between the pressure tap and nozzle exit, (Fig. 10) yields:

$$\frac{P_1}{\gamma} + \frac{u_1^2}{2g} = \frac{u_0^2}{2g} \quad (1)$$

where:  $P_1$ ,  $u_1$  = Gage pressure and mean velocity at pressure tap

$u_0$  = jet exit mean velocity

$g$  = acceleration of gravity

$\gamma$  = specific weight of water.

Rearranging (1):

$$u_0^2 = u_1^2 + \frac{2P_1}{\rho} \quad (2)$$

From conservation of mass:

$$u_1 A_1 = u_0 A_0 \quad (3)$$

where:  $A_1$ ,  $A_0$  = cross sectional area at pressure tap and nozzle exit, 0.781 in.<sup>2</sup> and 0.125 in.<sup>2</sup>.

Substituting (3) into (2):

$$u_0 = \left[ \frac{2P_1 A_1^2}{\rho (A_1^2 - A_0^2)} \right]^{1/2} = 1.03 P_1^{1/2} \quad (4)$$

### 2. Bucket

Definitions:

$d_0$  = Nozzle exit diameter

$F_{th}$  = Thrust available at bucket =  $2mu_2$



$F_i$  = Thrust available at nozzle exit =  $2mu_0$   
 $F_m$  = Measured thrust  
 $F_{max}$  = Maximum measured thrust  
 $l$  = Nozzle straight section length  
 $\eta_B$  = Bucket efficiency =  $F_m/F_{th}$   
 $m$  = Mass flow rate  
 $u_2$  = Mean jet velocity entering bucket  
 $u_3$  = Mean jet velocity leaving bucket  
 $x$  = Nozzle to bucket distance.

Therefore,

$$\frac{u_2}{u_0} = \frac{F_{th}}{F_i} = \frac{F_m}{\eta_B F_i} \quad (5)$$

The thrust available at the nozzle exit is:

$$F_i = 2m_0 u_0 = 2\rho A_0 u_0^2 = 0.514 P_1$$

Substituting for  $F_i$  in Eq. (5):

$$\frac{u_2}{u_0} = \frac{F_m}{0.514 \eta_B P_1} \quad (6)$$

Equation (5) only applies to a coherent jet where the amount of spray is small so that  $m$  = constant. This fine, low density spray was noted by Leach and Walker [Ref. 2] and is clearly shown in their x-ray and diffused lighting photographs. Farmer and Attewell [Ref. 3] also noted the "vapour cloud" surrounding the solid core of a coherent water jet.



For small distances from the nozzle,  $u_2 \approx u_0$ , thus giving an estimate of the bucket efficiency,

$$\eta_B \approx \frac{F_{\max}}{F_1} \quad (7)$$

Assuming  $\eta_B$  is constant,  $u_2/u_0$  may be further simplified to:

$$\frac{u_2}{u_0} = \frac{F_m}{F_{\max}} \quad (8)$$

## B. NOZZLE OPTIMIZATION

Data obtained for the nozzle optimization runs was put in nondimensional form by expressing the distance from the nozzle and the length of the straight portion of the nozzle in terms of nozzle diameters. This gives a range of distances from 2 to 246 nozzle diameters, and a range of nozzle length from 1 to 11 diameters, based upon the nozzle diameter of 0.400 in. Relative performance was expressed by the ratio of the thrust obtained at a given position ( $F_m$ ) to the maximum thrust ( $F_{\max}$ ) obtained for that nozzle length. In all cases except the zero length nozzle, the maximum thrust occurred at the nozzle exit. Since some runs fell below the 500 psi desired, all data was processed for 480 psi.

The data was found to have considerable variation for some runs at distances greater than 150 diameters. This was considered to be due to two factors: the increasing difficulty in aligning the bucket with the jet at longer



distances, and the jet breakup and spreading which would cause incomplete turning of the jet by the bucket. In some instances an attempt was made to repeat these particular runs with better alignment, but this usually yielded only marginal improvement and was a costly procedure in terms of nitrogen gas supply. Additionally, for the runs concerned, the jet was of generally poor quality so that the data for these regions would not be particularly useful for application to a propulsive jet.

Testing was begun with a nozzle length of seven diameters, but as data was accumulated, it became apparent that performance was gradually decreasing as the nozzle was shortened. Therefore, a second nozzle with a straight section length of 10.95 diameters was made up to cover a wider range of  $l/d_0$ . The second nozzle was made to match the first as closely as possible. Time did not permit testing this nozzle for any length less than eight diameters.

To put the data in a usable form, smooth curves of the performance had to be constructed. A computer curve fitting routine such as the least squares method was considered, but the difficulty of assigning proper weighting factors to each data point could not be resolved. Therefore, curves were fitted to the data manually. In doing this, the difficulty of bucket alignment at large  $x/d_0$  was taken into account by giving greater credence to the higher values of thrust that occurred.

Although data was obtained for a zero nozzle length, it was not used in assembling the results because a higher





value of thrust was produced at  $x/d_0 = 28$  than at the nozzle. At distances greater than 28 diameters, thrust was again lower and, in general, performance was poor. The effect of an increasing, then decreasing thrust as the bucket was moved away from the nozzle is due to the formation of a vena contracta near the nozzle.

Figures 11 and 12 present the relative performance ( $F_m/F_{max}$ ) and the performance ( $F_{th}/F_i$ ) using Eq. (6) versus the nozzle to bucket distance. Results for even-numbered nozzle lengths are used as a representative set, rather than attempting to show all the values obtained. The variations, or scatter of data mentioned previously, are apparent in both of these plots. To compute the performance shown in Fig. 12, a bucket efficiency of 86.7 per cent was used. This was computed from Eq. (7) and was the highest value of  $\eta_B$  obtained for all the testing done. It occurred for a nozzle length of one diameter, which is consistent with the fact that pipe drag losses will be lowest in the shortest length nozzle.

Figure 13 illustrates the effect of nozzle length on the thrust achieved at the nozzle exit compared to the thrust ideally available ( $F_{max}/F_i$ ). As would be expected, this ratio is reduced for longer nozzle lengths, in accordance with pipe drag theory. On this basis, it would be preferable to use the shortest nozzle straight section length consistent with good jet quality when selecting a particular nozzle configuration for propulsive water jet applications.



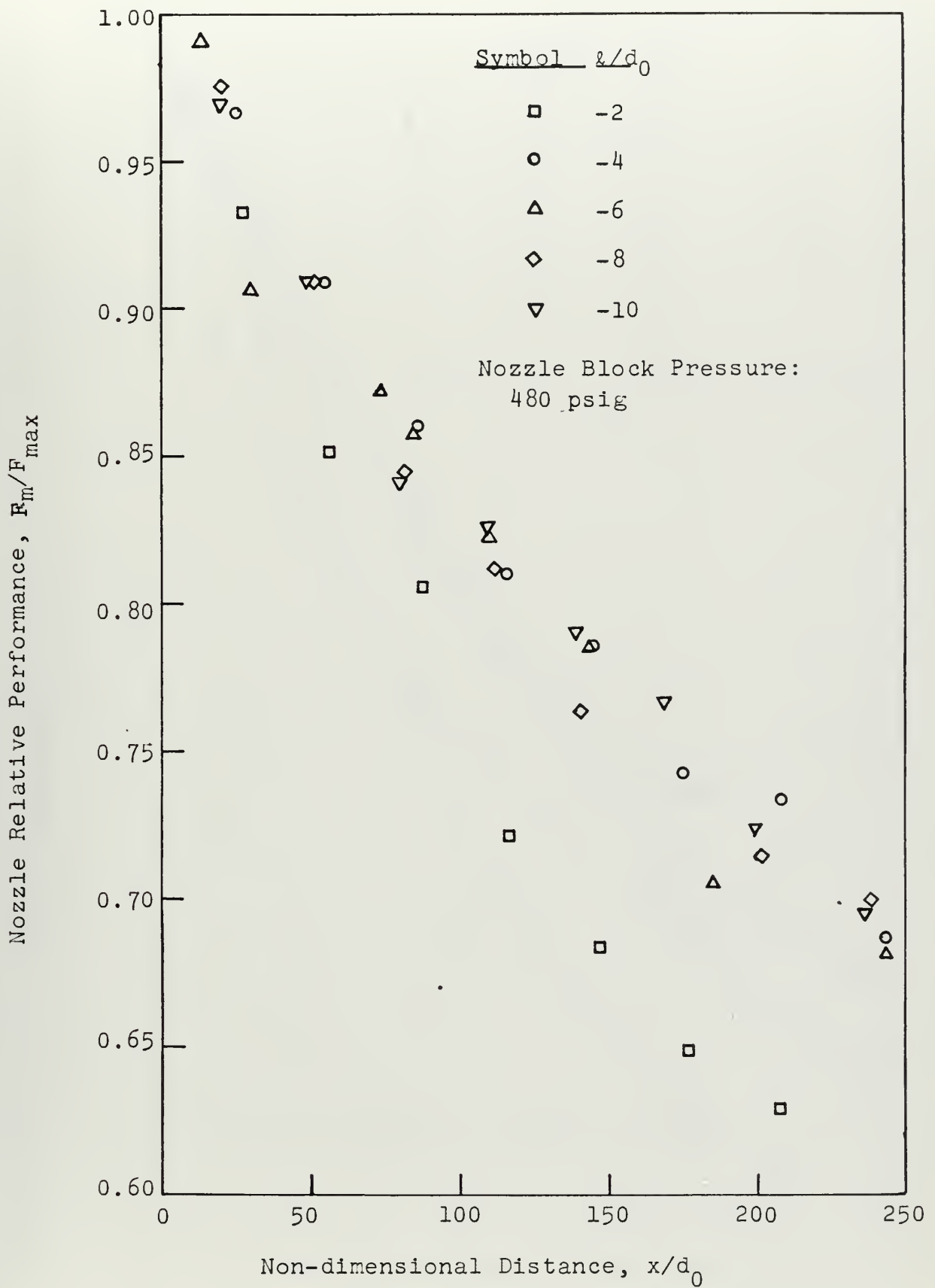


Fig. 11: Nozzle Optimization Data, Even Numbered Runs.



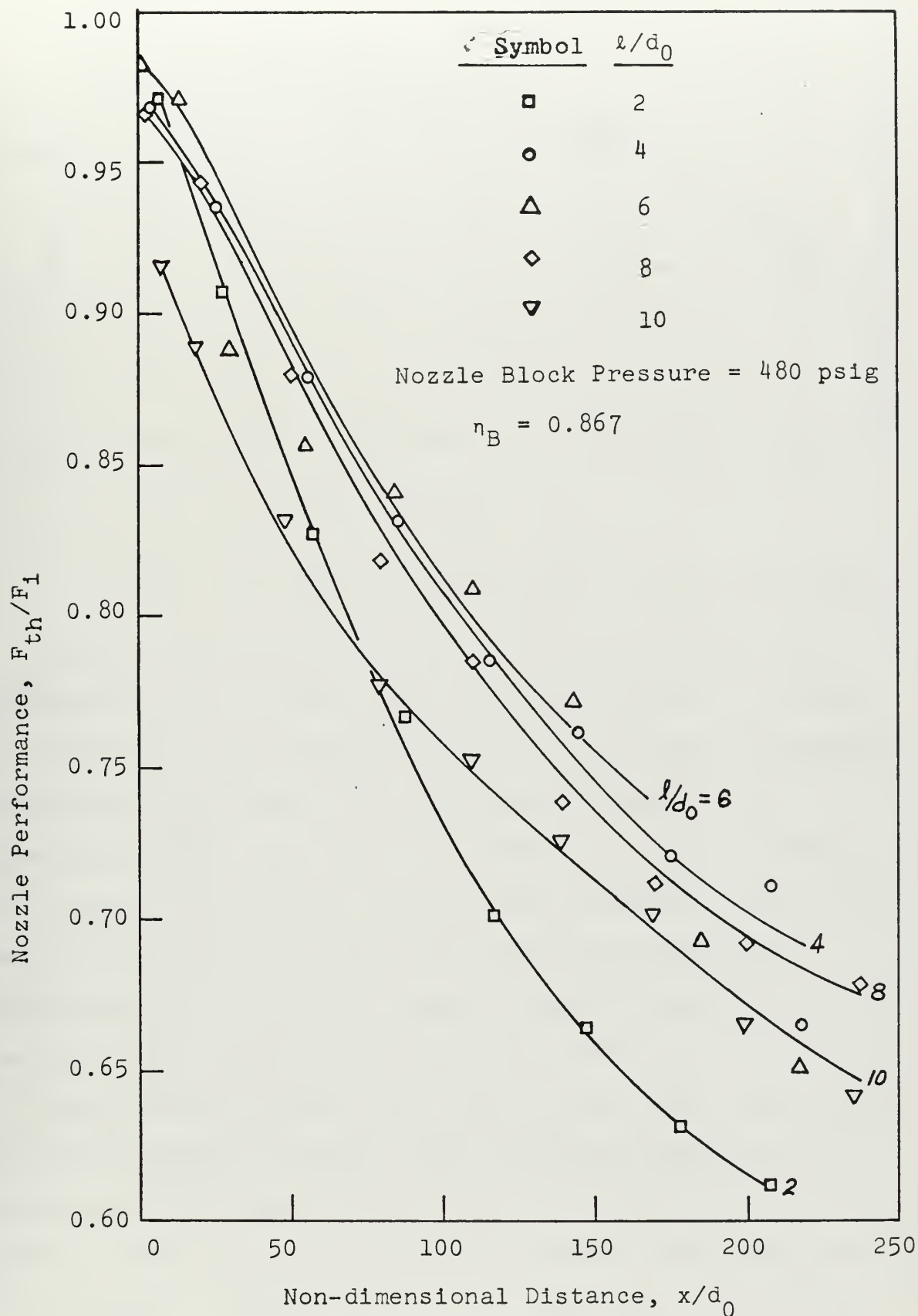


Fig. 12: Nozzle Performance Adjusted for Bucket Efficiency, Even Numbered Runs.



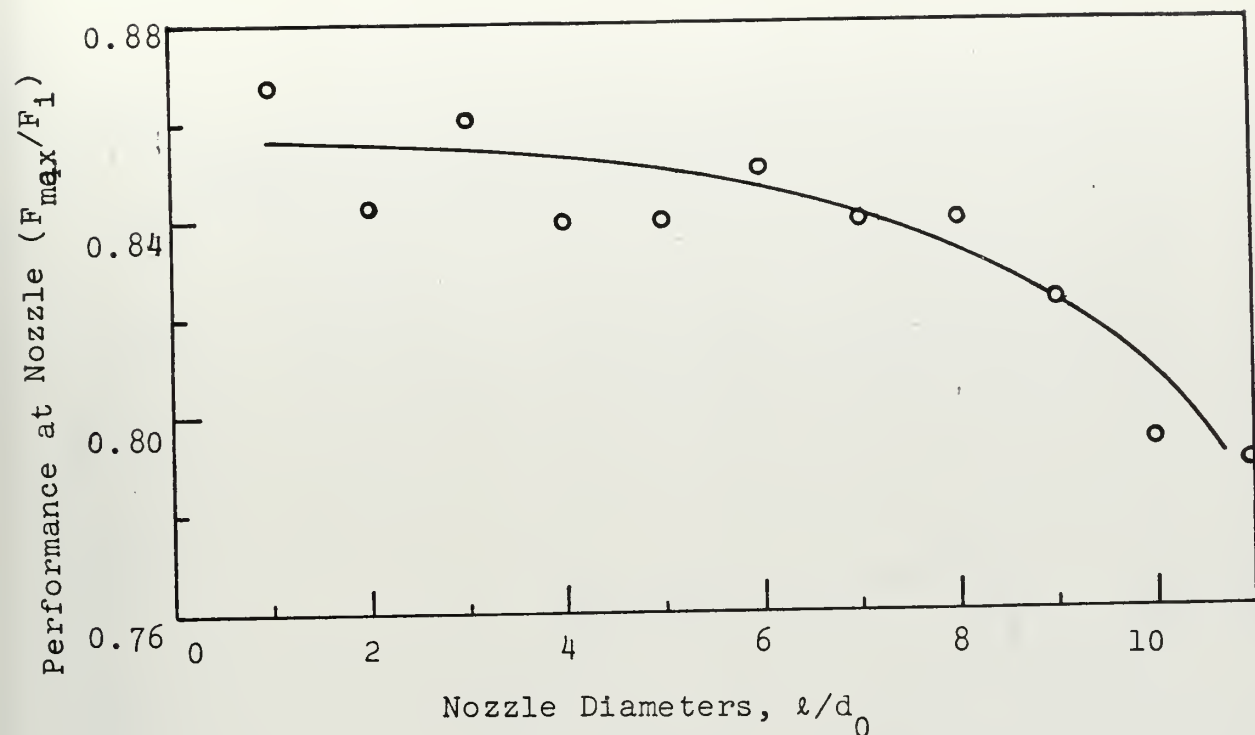


Fig. 13: Variation in  $F_{\max}/F_1$  at the nozzle exit.

Figure 14 shows the overall trend of performance with increasing length of the nozzle straight section. Increasing performance was obtained up to  $l/d_0 \approx 4$  with a leveling off through the range of four to eight diameters, then a gradual decrease up to  $l/d_0 = 11$ . Not too much confidence is attached to the peak shown at seven diameters, since this was the first data run made. The experience gained in operating the test facility gives increased confidence in the data accumulated during subsequent testing.

These results differ from those of Leach and Walker [Ref. 2] in two respects. First, their peak performance for a nozzle length of two to four diameters did not occur in the present study. Second, performance remains relatively good in the range of four through seven diameters, whereas their results show a rapid decline for lengths longer than four





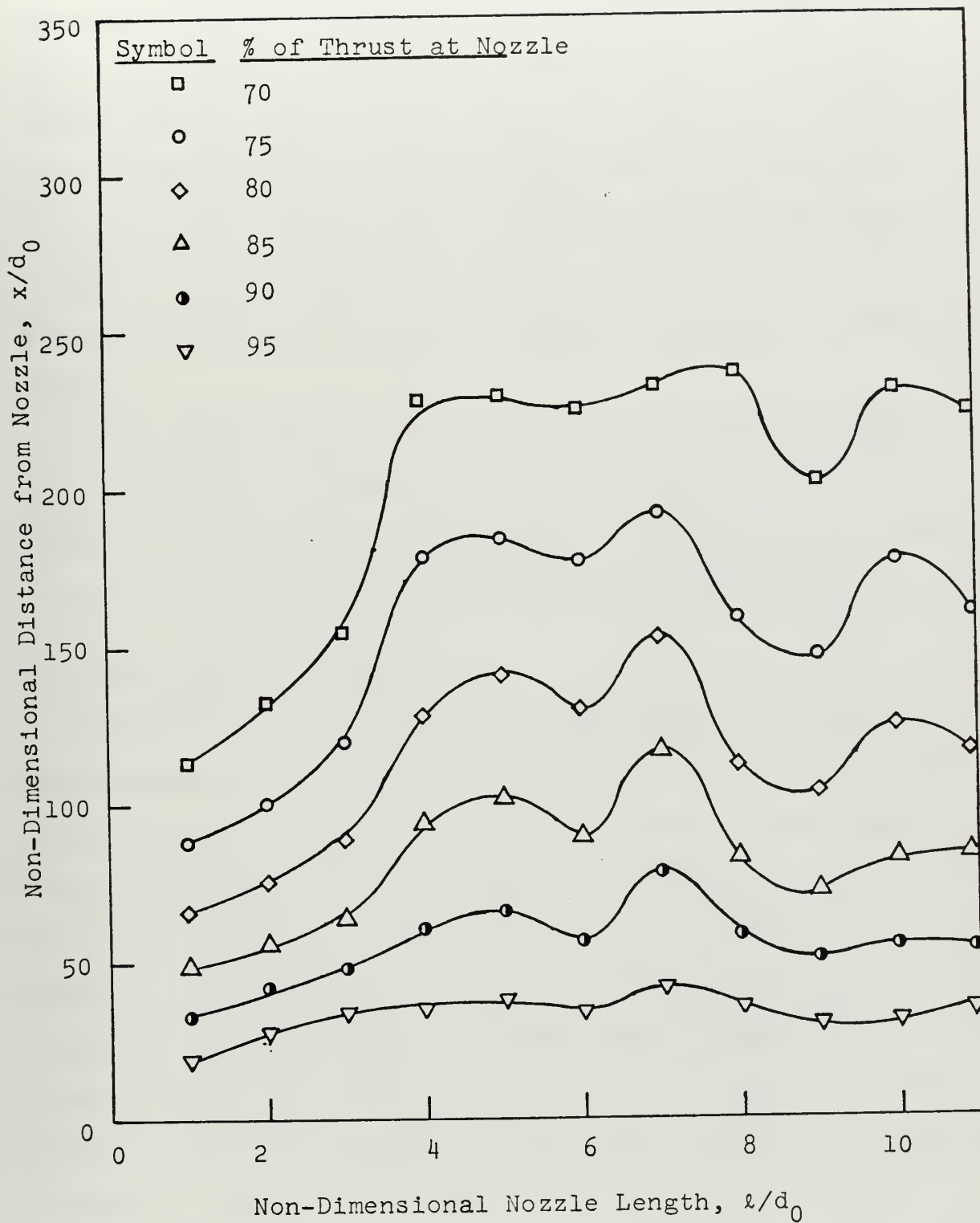


Fig. 14: Overall Performance Curves Showing the Effect of Nozzle Length on Jet Thrust Loss ( $F_m/F_{max}$ ).



diameters. The difference in the results is thought to be partly due to a higher level of turbulence in the flow arriving at the nozzle for the present study. Thus the longer nozzle lengths may be acting as a quieting section for the water before it leaves the nozzle. Confirmation of this could be achieved in future studies by providing a longer constant diameter section before the nozzle or by inserting honeycomb material to reduce the scale of turbulence.

With respect to the best performance achieved in each study, Leach and Walker obtained 75 per cent of the nozzle pressure at a distance of about 175 to 180 diameters, which is in agreement with the present study as seen in Fig. 14.

### C. PHOTOGRAPHIC RESULTS

Photographs of the water jet were taken to assist in illustrating the differences between the jet coherence for various nozzle lengths. Figures 15 through 17 are representative of the results obtained. As previously mentioned, in normal lighting the jet appears to be a disintegrated spray as seen in Fig. 15. Strong, diffused backlighting allows photographing only the dense core of the jet as shown in Figs. 16 and 17. Direction of jet travel is from right to left. The center of the field of view is at approximately 30 diameters distance from the nozzle and spans a length of about 50 diameters. The jet of Fig. 16 is of good quality and is about three-fourths in. in diameter at its narrowest part while that of Fig. 17 is of poor quality and



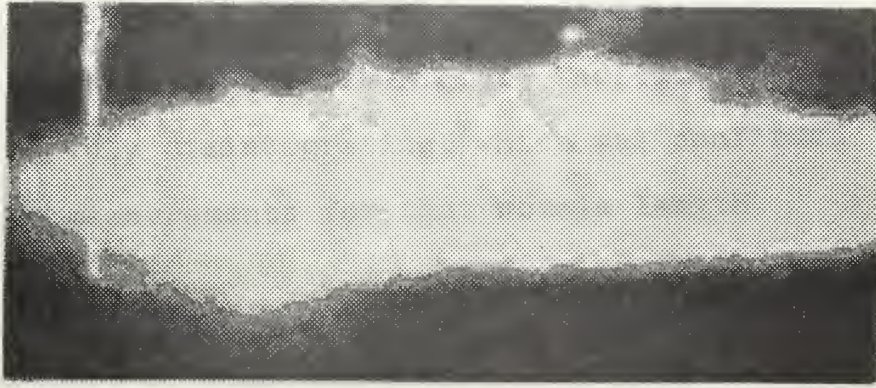


Fig. 15: Typical Appearance of Jet in  
Normal Lighting:  $\ell/d_0 = 6$ .  
Camera:  $1/200$  sec,  $f\ 4.7$ .

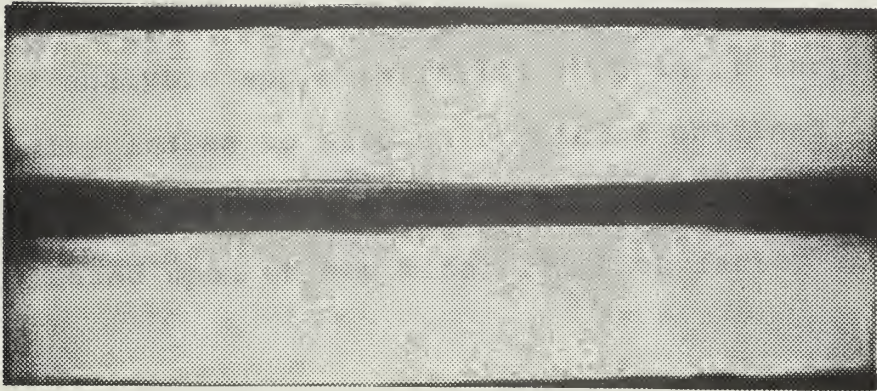


Fig. 16: Core of a Coherent Jet;  $\ell/d_0 = 10.95$ .  
Camera:  $1/500$  sec,  $f\ 4.7$ .

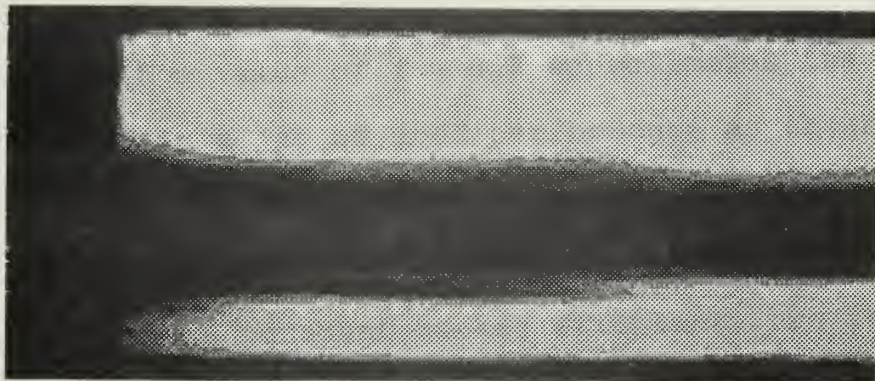


Fig. 17: Core of Low Performance Jet;  $\ell/d_0 = 0$ .  
Camera:  $1/500$  sec,  $f\ 4.7$ .





is about two in. wide in the core. The fairly dense region surrounding the core in Fig. 17 indicates that the jet is rapidly disintegrating, which was confirmed by the thrust measurements for that nozzle length.

#### D. ANALYTICAL RESULTS

One objective of this study was to develop an analytical model to predict the velocity loss with increasing distance from the nozzle exit. The expressions derived and their development are contained in Appendix A.

A purely analytic approach failed to predict large enough velocity losses to account for those obtained experimentally. Therefore, a simple mathematical model was derived based upon an empirical friction factor as follows:

$$\frac{u}{u_0} = \left[ 1 + \frac{\rho_A}{\rho_W} f \frac{x}{d_0} \right]^{-2}$$

where:  $f = \text{constant}$ .

It was found that a value of  $f = 0.7$  approximates the velocity falloff in a jet of good performance as shown in Fig. 18. The experimental values shown are for a nozzle length of five diameters and are computed using Eq. (8). A coherent jet and a constant bucket efficiency are thus assumed to allow making this calculation. However, based upon the performance at  $l/d_0 = 5$ , this assumption appears to be valid. Good coherence was confirmed visually for the first two-thirds of the jet length during testing, and it is also evident in the photographs taken.





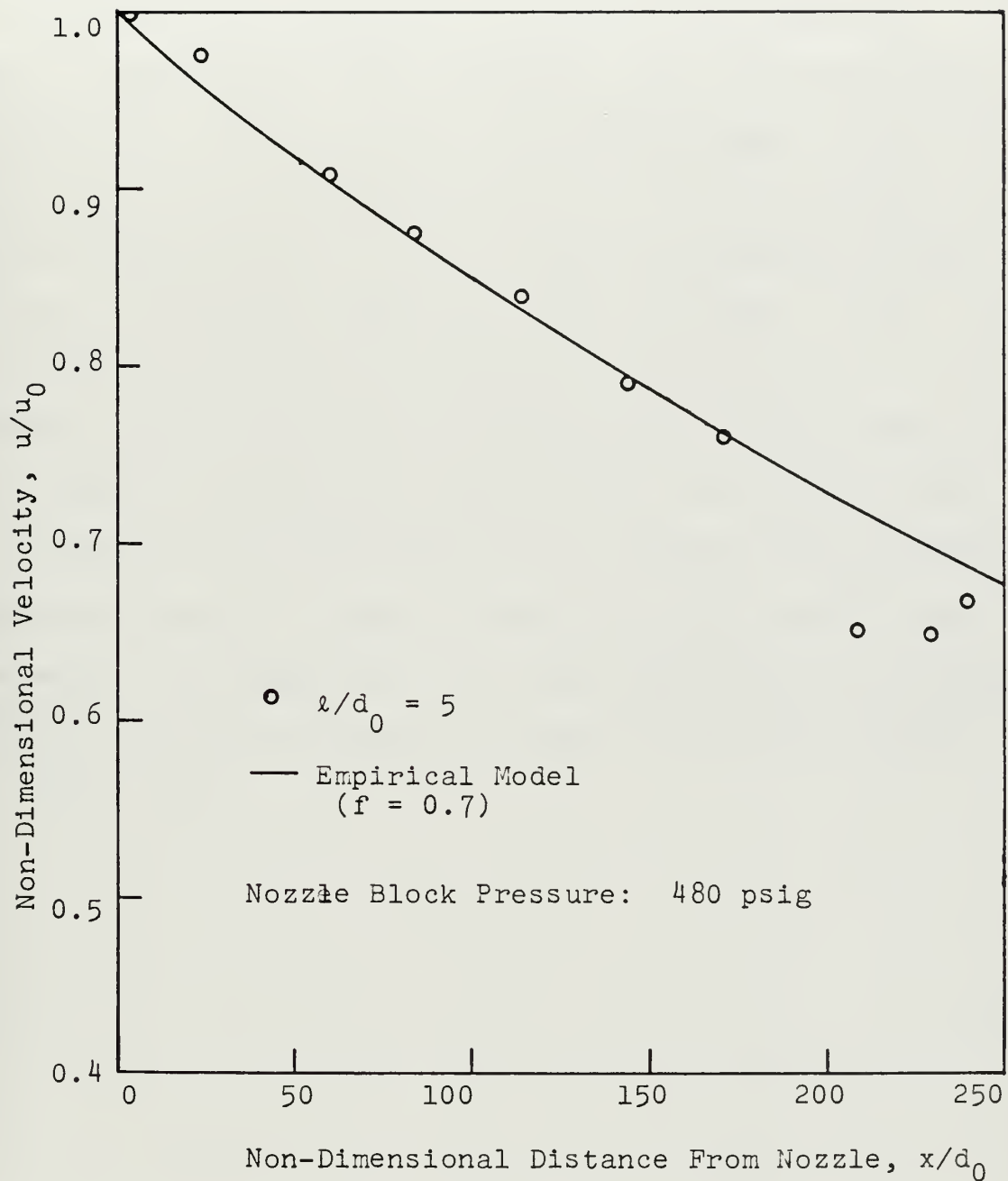


Fig. 18: Comparison of Data With Empirical Model



As a result of the analysis done, it appears that a very high friction factor applies, especially when typical values of  $f$  for pipe flow are in the vicinity of 0.05. It is evident that the phenomenon involved in the turbulent shear on a water jet is very different from that operating in other types of flow. Part of the reason that  $f$  is so high is that it is multiplied by the ratio of air density to water density ( $\approx 1.2 \times 10^{-3}$ ). Thus, to account for the high rate of velocity reduction,  $f$  must be large. It is also possible that because of the spray that exists, a different density ratio would be appropriate in this case.

It must be stressed that the friction factor of 0.7 can only be applied for the limited study completed ( $Re_{d_0} = 8.45 \times 10^5$ ). Further testing for a range of Reynolds number must be done to determine the variation of  $f$ . Only then can the use of the relation developed be extended to other situations of free jet velocity loss.



## VII. SUMMARY

### A. CONCLUSIONS

The following conclusions can be made based upon the experimental data developed and the investigation conducted.

1. Previous research of the nozzle designs required to produce coherent high velocity water jets has found that the cone and cylinder profile is best suited for this purpose.
2. The results of the present study show that, for the nozzle tested ( $17.8^\circ$  cone angle, 0.400 in. exit diameter, 0.957 in. inlet diameter) the optimum length of the nozzle straight section following the cone is about four to five nozzle diameters. This does not agree with the optimum length of two to four diameters recommended in the literature.
3. For application of the nozzle design tested to the transit system proposed by Beckwith [Ref. 1], the curves of Fig. 14 can be used to predict the maximum distance allowable between buckets. If, for example, a 25 per cent loss in thrust can be allowed, bucket spacing should be no more than 185 diameters or 74 in. This requires 33 buckets for a 200 ft long vehicle. For allowable 10 per cent thrust loss, spacing should be no more than 65 diameters or 26 in., which requires 93 buckets for the same vehicle. However, since the



curves were developed for a pressure of 480 psig, they may not be valid for the transit system design pressure of 3620 psig.

4. An empirical model was developed which predicts the velocity reduction with increasing standoff distance from the nozzle tested and at the Reynolds number for the investigation. A friction factor of 0.7 was found to give correlation with the data. The use of this relation is restricted to the present case until further correlations are made.
5. The test facility constructed is adequate in durability but somewhat inconvenient to use.

#### B. RECOMMENDATIONS

To improve upon the validity of the present study and to investigate other areas of interest, the following recommendations are pertinent:

1. Extend the performance and optimization study to higher pressures.
2. Improve the capabilities of the test facility as follows:
  - a. Provide a solenoid operated cutoff valve as near the reservoir as practicable to conserve the gas supply.
  - b. Either redesign the bucket to provide higher efficiency, or modify the system to record jet stagnation pressure.
  - c. Redesign the spray covers to reduce annoying water leakage.





- d. Provide a means of reducing the scale of turbulence of the flow entering the nozzle either by honeycomb material or a longer constant diameter section.
  - e. Provide more precise bucket positioning control by the use of jack-screws. This would also reduce time between runs, but might reduce capabilities in terms of strength.
- 3. Investigate the effects of nozzle to bucket angular misalignment as might occur on curved portions of the proposed transit system.
  - 4. Investigate the possible benefits of polymer solutions in terms of jet coherence as well as decreased pipe drag and bucket flow losses.
  - 5. Obtain high speed motion pictures of the jet to study the mechanisms of jet disintegration. The results of this study might lead to a more precise formulation of the velocity loss of a high velocity free jet.



## APPENDIX A - JET VELOCITY LOSS ANALYSIS

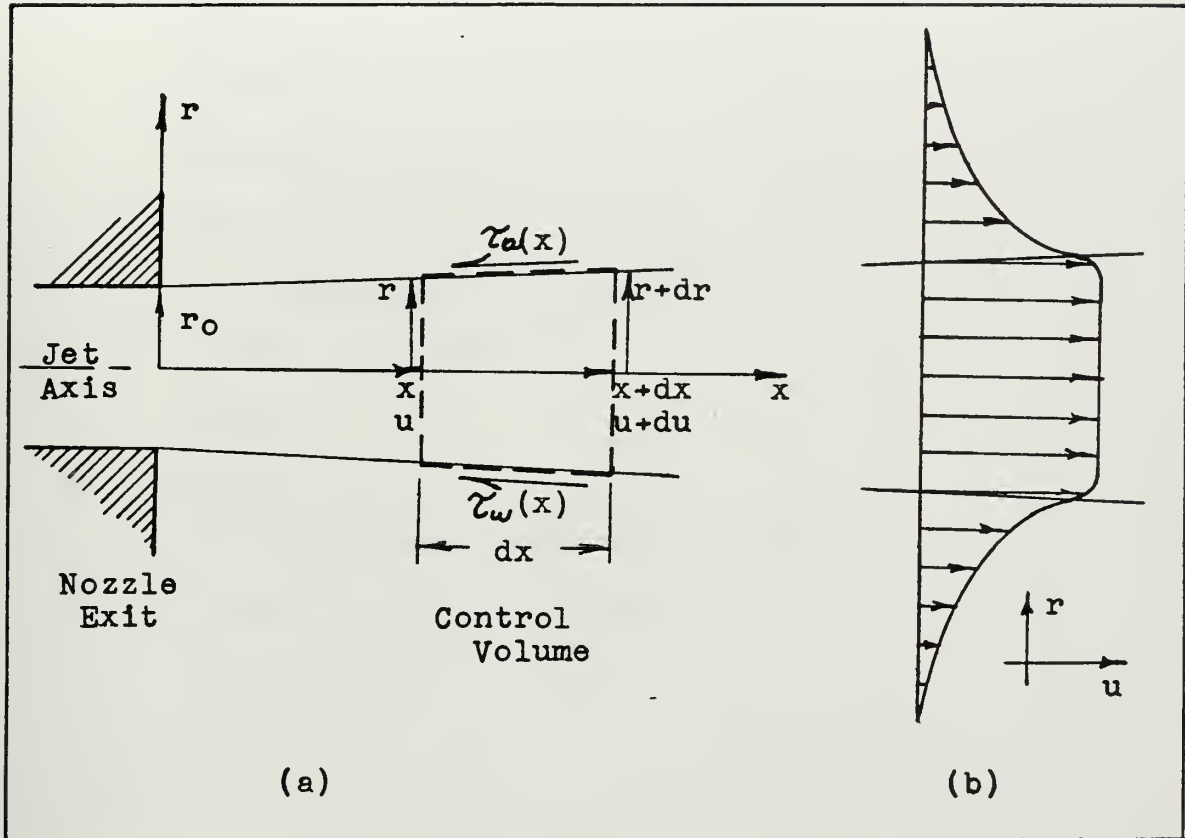


Fig. A-1: (a) Water Jet Control Volume  
(b) Assumed Velocity Profile

### A. LIST OF SYMBOLS AND DEFINITIONS

$A_1, A_2$	Simplifying combinations of constant properties
$C_1, C_2$	Constants of integration
$c_f'$	Local coefficient of skin friction
$c_f$	Total coefficient of skin friction
$d$	Diameter
$f$	Friction coefficient
$k_s$	Equivalent sand roughness
$L$	Total length of jet
$m$	Mass flow rate



$x, r$	Axial and radial distances
$u$	Mean velocity in x-direction
$U_{\infty}$	Mean velocity in x-direction at $r = \infty$
$\rho$	Density
$\nu$	Kinematic viscosity
$\tau$	Shear stress

#### Subscripts, Superscripts

O	Value at nozzle exit
A	Air
W	Water
*	Nondimensional parameter or form
w	Value at wall or boundary
x	x-direction

### B. ASSUMPTIONS AND LOGIC

1. Turbulent fully developed flow within fluid as it leaves the nozzle; therefore a nearly flat velocity profile and  $u = u(x)$ ;  $\partial u / \partial r \approx 0$ . The simplification resulting from this assumption leads to a first order approximation for the rate of jet growth near the nozzle exit.
2. Coherent jet with insignificant spray loss; therefore primary losses due to shear on water boundary.
3. A free jet; therefore pressure is constant and control volume is in equilibrium with respect to pressure forces.
4. Velocity decreases with increasing  $x$ ,  $\partial u / \partial x < 0$ .



5.  $\rho_W, \rho_A, v_W, v_A$  are constant.

6. Insignificant loss to spray and constant  $\rho_W$  requires that jet enlarges with decreasing velocity, therefore  $r = r(x)$ .

### C. JET RADIUS-VELOCITY RELATIONSHIPS

Applying conservation of mass to the control volume in Fig. A-1:

$$m = \pi \rho_W r^2 u = \pi \rho_W r_0^2 u_0$$

$$r = r_0 \left( \frac{u_0}{u} \right)^{1/2} \quad (1)$$

$$dr = -1/2 u_0^{1/2} r_0 u^{-3/2} du \quad (2)$$

### D. FORCE-MOMENTUM BALANCE

Applying conservation of momentum:

$$\begin{aligned} \Sigma \text{ Forces}_x &= \Delta \text{ Momentum}_x \\ -\tau_W(2\pi r dx) &= -mu + m(u + du) \\ &= -(\rho_W \pi r^2 u)(u) + [\rho_W \pi (r+dr)^2 (u+du)][u+du] \end{aligned}$$

Dropping higher order terms and products:

$$-\frac{\tau_W}{\rho_W} dx = r u du + u^2 dr$$

Substituting (1) and (2) for  $r, dr$ :

$$-\frac{\tau_W}{r_0 \rho_W} dx = 1/2 u_0^{1/2} u^{1/2} du$$

$$u^{1/2} du = \frac{-2\tau_W}{r_0 \rho_W u_0^{1/2}} dx \quad (3)$$





## E. EVALUATION OF SHEAR STRESS

### Assumptions:

1. Overall flow can be considered to be analogous to the case where the jet is stationary and air at  $r = \infty$  is moving at a velocity of  $u(x)$  to the left.
2. Considering the jet boundary as a "solid" surface,  $\tau_w(x)$  can be approximated by established results for turbulent flow over a plate at zero incidence.

Relationships from Schlichting [Ref. 9] give  $\tau_w$  for turbulent flow over smooth and rough plates which can be applied if  $(L-x)$  is used as the distance parameter to allow  $\tau_w$  to be a maximum at the end portion of the jet and a minimum at the nozzle. This is because the  $x$ -coordinate direction used to describe the flow for the flat plate is the reverse of that being used in this analysis for the same direction of air flow. These relations for  $\tau_w$  apply within a limited range of Reynolds numbers, namely  $5 \times 10^5 < Re_L < 10^7$ . Here  $Re_L = \frac{U_\infty L}{\nu}$ , where  $U_\infty$  = free-stream velocity,  $L$  = length of plate over which the fluid acts, and  $\nu$  = kinematic viscosity of the fluid. However, it is pointed out by Hoerner [Ref. 10] that agreement is good up to  $Re_L \approx 5 \times 10^8$  and can probably be extended up to  $10^{10}$  without extensive error.



## F. SMOOTH JET BOUNDARY

Taking first the case of the smooth plate:

$$c_f' = \frac{\tau_w}{1/2 \rho U_\infty^2} = 0.0592 (Re_x)^{-1/5}$$

where  $c_f'$  is the local skin friction coefficient.

Substituting  $(L-x)$  for the length and allowing the velocity to be a variable corresponding to that locally found in the jet:

$$\tau_w = 0.0296 \rho_A u^2 \left[ \frac{v_A}{u(L-x)} \right]^{1/5}$$

$$\tau_w = 0.0296 \rho_A u^{9/5} v_A^{1/5} (L-x)^{-1/5} \quad (4)$$

Application of (4) to (3) yields a differential equation in  $u$  and  $x$ :

$$u^{-13/10} du = - \frac{2}{r_0 \rho_w u_0^{1/2}} 0.0296 \rho_A v_A^{1/5} (L-x)^{-1/5} dx$$

integrating

$$u^{-3/10} = -A_1 (L-x)^{4/5} + C_1$$

where

$$A_1 = \frac{0.0222}{r_0 u_0^{1/2}} \frac{\rho_A}{\rho_w} v_A^{1/5}$$

The boundary condition is:

$$x = 0, u = u_0.$$

Applying the boundary condition,  $C_1$  is evaluated, giving:

$$u^{-3/10} = u_0^{-3/10} + A_1 [L^{4/5} - (L-x)^{4/5}] \quad (5)$$



It is noted that this expression requires that the distance  $L$  approach  $\infty$  for the jet velocity to approach zero, owing to the decreasing shear acting upon it. If, for example, the integration had been executed using a constant shear value, then the jet could come to rest at a finite distance. It should also be pointed out that, because of the assumption of no mass loss, yet a decreasing velocity, Eq. (1) requires that the jet radius approach an infinite size to allow the velocity to approach zero. However, since the analysis is not expected to be applied at long distances, these unrealistic conditions of the relations developed are not relevant.

Equation (5) is non-dimensionalized by introducing the following parameters:

$$u^* = \frac{u}{u_0} ; \quad x^* = \frac{x}{d_0} ; \quad L^* = \frac{L}{d_0}$$

which yields upon rearranging:

$$u^* = \left[ 1 + 0.0444 (\text{Re}_{d_0})^{-1/5} \frac{\rho_A}{\rho_W} \left[ \frac{v_A}{v_W} \right]^{1/5} L^{*4/5} \left[ 1 - \left( 1 - \frac{x^*}{L^*} \right)^{4/5} \right] \right]^{-10/3} \quad (6)$$

To evaluate this equation, an overall jet length must be specified and the limits on  $x$  are then from zero to that length. For a given set of physical properties the variables are the Reynolds numbers based upon the initial jet diameter, the overall travel of the jet,  $L^*$ , and the distance downstream,  $x^*$ .

For lack of a clear cut criterion, Eq. (6) was evaluated on the basis of the nozzle velocity attained in the



present study (279 ft/sec) and the Reynolds number ( $Re_x$ ) of  $10^{10}$ . This yields a permissible length of jet travel,  $L^*$ , of 832 diameters for the nozzle diameter of 0.400 in., and calculations were therefore made using  $L^* = 1000$ . Owing primarily to the low density of air, the model predicts only a 0.5 per cent velocity dropoff at  $x^*/L^*=1.0$ . This formulation then is obviously of no value in predicting velocity decrease in a coherent jet.

#### G. ROUGH JET BOUNDARY

Turning now to the supposition that the boundary of the coherent jet is not smooth, but ruffled by the shear action of the air moving relative to it, relationships for the skin friction coefficient for turbulent flow over rough surfaces are applied. This introduces yet another variable; the degree of equivalent sand roughness,  $k_s$ . Taking the relationships presented by Schlichting [Ref. 9] for  $c_f'$  and  $c_f$ ;

$$c_f'(x) = \left[ 2.87 + 1.58 \log \frac{x}{k_s} \right]^{-2.5} \quad (7)$$

$$c_f(L) = \left[ 1.88 + 1.62 \log \frac{L}{k_s} \right]^{-2.5} \quad (8)$$

we again apply the distance substitution of  $(L-x)$  to allow for the difference in x-coordinate direction. Substitution of  $c_f'$  for  $\tau_w$  in Eq. (3) and showing the integration limits on  $u$  and  $(L-x)$  yields

$$\int_{u_0}^u u^{-3/2} du = \frac{1}{r_0 u_0^{1/2}} \frac{\rho_A}{\rho_W} \int_L^{(L-x)} c_f'(L-x) dx \quad (9)$$





By integration of (9),

$$u_0^{-1/2} - u^{-1/2} = - \frac{1}{r_0 u_0^{1/2}} \frac{\rho_A}{\rho_W} c_f (L-x) \quad (10)$$

Rearranging and putting in dimensionless form,

$$u^* = \left[ 1 + 2 \frac{\rho_A}{\rho_W} x^* c_f^* \right]^{-2} \quad (11)$$

where:

$$c_f^* = \left[ 1.89 + 1.62 \log \frac{d_0}{k_s} L^* \left[ 1 - \frac{x^*}{L^*} \right] \right]^{-2.5}$$

Again it is seen that a jet length must be specified to determine the effect of the air flow on the assumed jet. An equivalent roughness must be specified and, in the form presented  $\frac{d_0}{k_s}$ , it can be expressed as a percentage of the initial jet diameter. Because of the cancellation of velocity terms, the form of Eq. (11) is independent of Reynolds number, which belies intuition. However, in accordance with Eqs. (7) and (8) the local and total skin friction coefficients are also independent of Reynolds number, being functions of distance and equivalent sand roughness only. By specifying an initial velocity,  $u_0$ , we are in effect applying a Reynolds number in the equation, but this is factored out in the non-dimensional form of Eq. (11).

Evaluation of Eq. (11) was done using non-dimensional jet lengths of  $L^* = 1000, 500$  and  $100$  diameters while varying the roughness factor in each of the three cases. An improvement was obtained over the smooth surface assumption,



but velocity decrease close to the nozzle was still very small compared to that actually found to take place. For example, at a distance of 100 diameters from the nozzle, with the jet length of 1000 diameters, and for a roughness of half the diameter, only four per cent reduction in velocity was predicted. The results are plotted in Fig. A-2 and it can be seen that only by using unrealistically long jet travel distances,  $L^*$ , could the dropoff in velocity be close to that actually occurring.

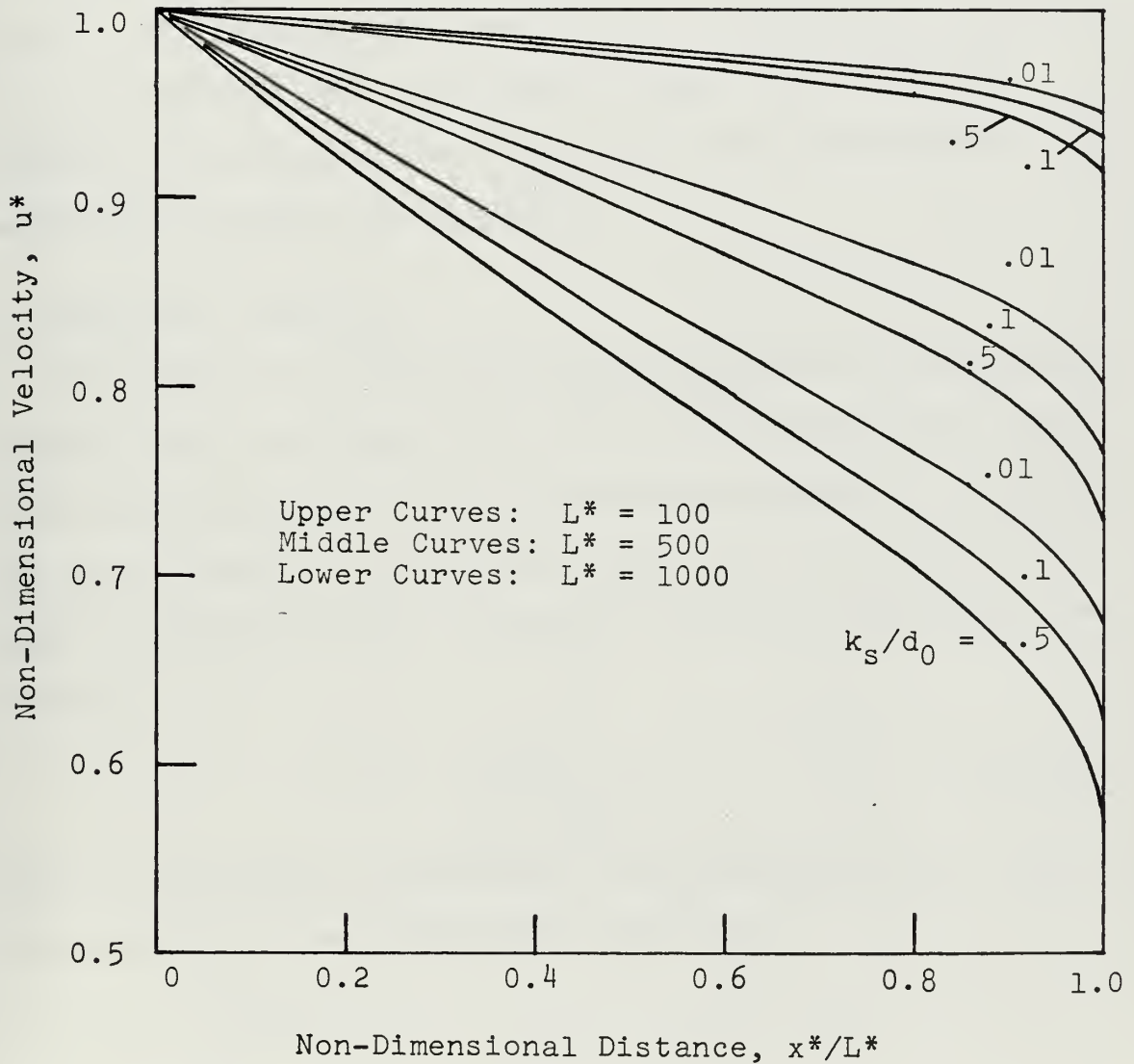


Fig. A-2: Velocity Decrease for Rough Jet



One possible method of making the above models predict the observed velocity decrease is to assume that the density of the fluid shearing the jet boundary is not that of air but that of some air-water spray mixture. However, this method is basically an even more empirical one, and still presents the difficulty of assigning an appropriate length of jet travel and, in the case of Eq. (11), a jet roughness. Additionally, the equations as developed are somewhat inconvenient to handle computationally, and they do not satisfy the objective of a simplified model of the jet velocity loss. Because of this, the analytical approach of obtaining the shear stress was abandoned and an empirical relation was attempted.

#### H. EMPIRICAL APPROACH

In a paper on liquid-vapor interactions in a condensing ejector, Levy and Brown [Ref. 11] successfully used a friction coefficient to predict some characteristics of a liquid jet acted upon by a surrounding high velocity steam flow. Adopting this approach, we define a friction coefficient as follows:

$$f = \frac{\tau_w}{1/2 \rho_A u^2} \quad (12)$$

where  $f$  is taken as a constant. Substitution of Eq. (12) in Eq. (3) yields the differential equation:

$$\int_{u_0}^u u^{-3/2} du = - \frac{2f}{u_0^{1/2} d_0} \frac{\rho_A}{\rho_W} \int_0^x dx$$



Integrating and rearranging,

$$\frac{u}{u_0} = \left[ 1 + \frac{\rho_A}{\rho_W} \frac{x}{d_0} \right]^{-2} \quad (13)$$

Introducing  $u^*$  and  $x^*$  as defined earlier:

$$u^* = \left[ 1 + A_2 x^* \right]^{-2} \quad (14)$$

where:

$$A_2 = \frac{\rho_A}{\rho_W} f$$

A comparison of Eq. (14) with Eq. (11) shows that they are of the same form, with  $f = 2C_f^*$ . The basic difference in the two relations is that  $f$  is assumed constant whereas  $C_f^*$  varied with roughness and distance.

Evaluation of Eq. (11) was accomplished for different values of  $f$ . Standard densities for air and water were used to compute  $A_2$ . The results are contained in Fig. A-3, and the velocity decrease with distance was found to be sufficient to bracket that actually measured in turbulent jets.





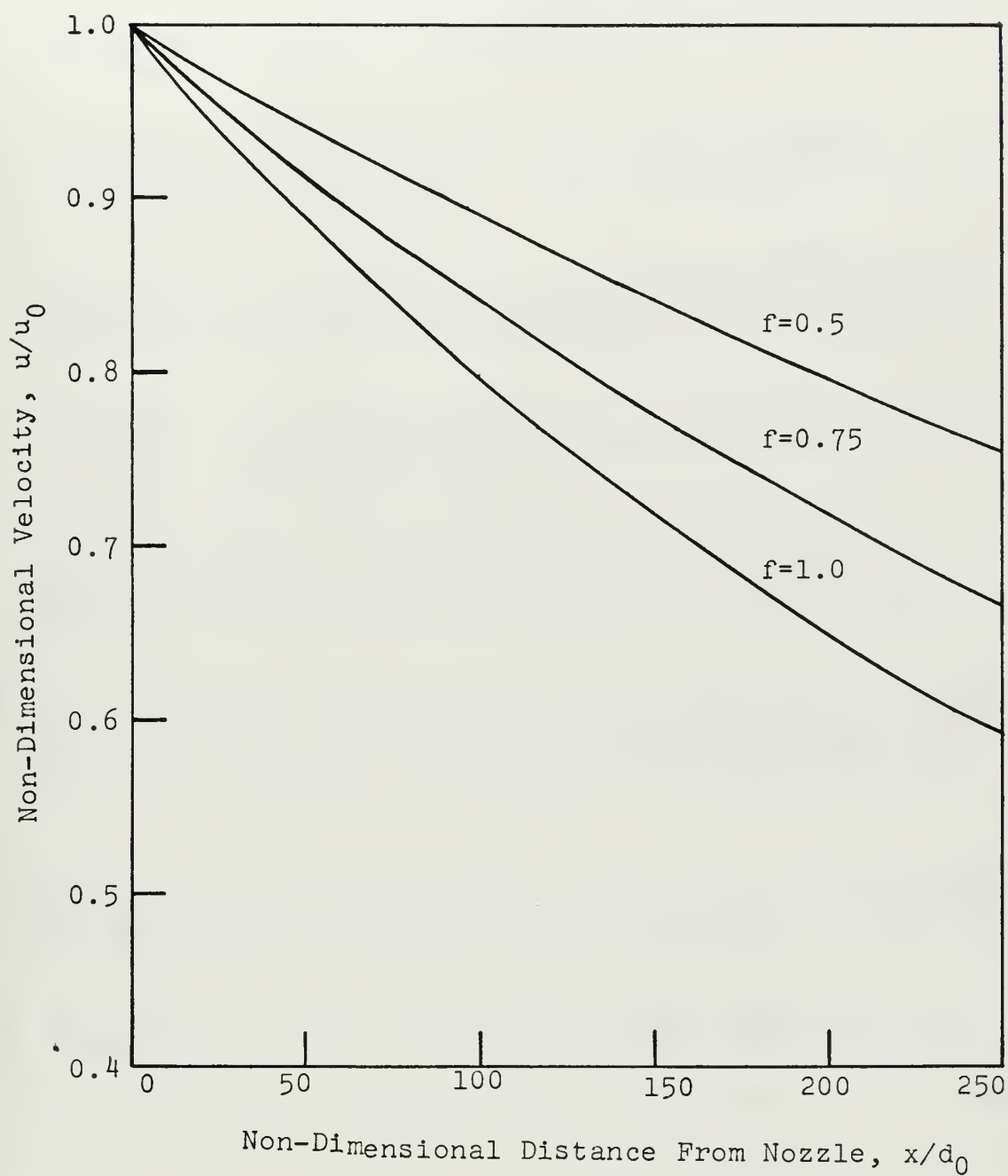


Fig. A-3: Empirical Model of Velocity Falloff



## BIBLIOGRAPHY

1. Beckwith, S., High-Speed Hydraulic Jet Propulsion for Urban and Interurban Transportation, ASME Paper No. 69-WA/PID-4, 1969.
2. Leach, S. J. and Walker, G. L., "Some Aspects of Rock Cutting by High Speed Water Jets", Philosophical Transactions of the Royal Society of London, v. 260, p. 295-305, 28 July 1966.
3. Farmer, I. W. and Attewell, P. B., "Rock Penetration By High Velocity Water Jet", International Journal of Rock Mechanics and Mining Science, v. 2, p. 135-141, 1965.
4. Palowitch, E. R. and Malenka, W. T., "Hydraulic Mining Research - A Progress Report", Mining Congress Journal, v. 50, p. 66-68, September 1964.
5. Harris, H. D., "Research into the Properties and Applications of High Energy Water Jets", National Research Council of Canada Quarterly Bulletin of the Division of Mechanical Engineering, p. 1-3, 6, June 1970.
6. Oak Ridge National Laboratory Report ORNL-HUD-1, UC-38, Contract No. W-7405-eng-26, Examination of High Pressure Water Jets For Use in Rock Tunnel Excavation, by W. C. McClain and G. A. Cristy, P. 6, 14-15, January 1970.
7. Rouse, H., Howe, J. W. and Metzler, D. E., "Experimental Investigation of Fire Monitors and Nozzles", Transactions of the American Society of Civil Engineers, v. 117, p. 1153-1162, 1171-1173, 1952.
8. Spannhake, Wilhelm, Centrifugal Pumps, Turbines, and Propellers, p. 309, Technology Press, 1934.
9. Schlichting, H., Boundary Layer Theory, 4th ed., p. 537-553, McGraw-Hill, 1960.
10. Hoerner, S. F., Fluid-Dynamic Drag, 2nd ed., p. 2-5, published by the author, 1957.
11. Levy, E. K. and Brown, G. A., Liquid-Vapor Interactions in a Constant-Area Condensing Ejector, ASME Paper No. 71-FE-21, 1971.



# INITIAL DISTRIBUTION LIST

	No. Copies
1. Defense Documentation Center Cameron Station Alexandria, Virginia 22314	2
2. Library, Code 0212 Naval Postgraduate School Monterey, California 93940	2
3. Professor R. H. Nunn, Code 59 Nn Department of Mechanical Engineering Naval Postgraduate School Monterey, California 93940	2
4. LCDR James Alexander Wilson, Jr. 10 Dublin Court Pleasant Hill, California 94523	1



## DOCUMENT CONTROL DATA - R &amp; D

(Security classification of title, body of abstract and indexing annotation must be entered when the overall report is classified)

1. ORIGINATING ACTIVITY (Corporate author)		2a. REPORT SECURITY CLASSIFICATION	
Naval Postgraduate School Monterey, California 93940		Unclassified	
2b. GROUP			
3. REPORT TITLE			
Some Characteristics of a Propulsive Water Jet			
4. DESCRIPTIVE NOTES (Type of report and inclusive dates)			
Master's Thesis, December 1971			
5. AUTHOR(S) (First name, middle initial, last name)			
James A. Wilson, Jr.			
6. REPORT DATE		7a. TOTAL NO. OF PAGES	7b. NO. OF REFS
December 1971		63	11
8a. CONTRACT OR GRANT NO.		9a. ORIGINATOR'S REPORT NUMBER(S)	
b. PROJECT NO.			
c.		9b. OTHER REPORT NO(S) (Any other numbers that may be assigned this report)	
d.			
10. DISTRIBUTION STATEMENT			
Approved for public release; distribution unlimited.			
11. SUPPLEMENTARY NOTES		12. SPONSORING MILITARY ACTIVITY	
		Naval Postgraduate School Monterey, California 93940	
13. ABSTRACT			
<p>To obtain a high velocity, coherent, propulsive water jet, proper nozzle design is required. Existing high performance nozzles are considered, and a selected design is tested to provide optimization and performance data in the form of velocity and thrust loss with increasing jet standoff. An expression is developed to predict the velocity loss using an empirical friction factor value determined from the data.</p>			





KEY WORDS	LINK A		LINK B		LINK C	
	ROLE	WT	ROLE	WT	ROLE	WT
Propulsive Water Jet						







Thesis  
W6375  
c.1

Wilson

133837

Some characteristics  
of a propulsive  
water jet.

Thesis  
W6375  
c.1

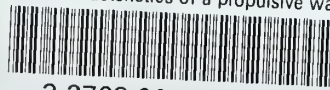
Wilson

133837

Some characteristics  
of a propulsive  
water jet.

thesW6375

Some characteristics of a propulsive wat



3 2768 001 90134 1

DUDLEY KNOX LIBRARY